1,8,10-Trisubstituted anthracenyl hydrocarbons: Towards versatile scaffolds for multiple-H-bonded recognition arrays

Silvia Forensi, Antoine Stopin, Federica de Leo, Johan Wouters, Davide Bonifazi

PII: S0040-4020(20)30449-X

DOI: https://doi.org/10.1016/j.tet.2020.131299

Reference: TET 131299

To appear in: *Tetrahedron*

Received Date: 2 April 2020

Revised Date: 15 May 2020

Accepted Date: 19 May 2020

Please cite this article as: Forensi S, Stopin A, de Leo F, Wouters J, Bonifazi D, 1,8,10-Trisubstituted anthracenyl hydrocarbons: Towards versatile scaffolds for multiple-H-bonded recognition arrays, *Tetrahedron* (2020), doi: https://doi.org/10.1016/j.tet.2020.131299.

Graphical abstract:

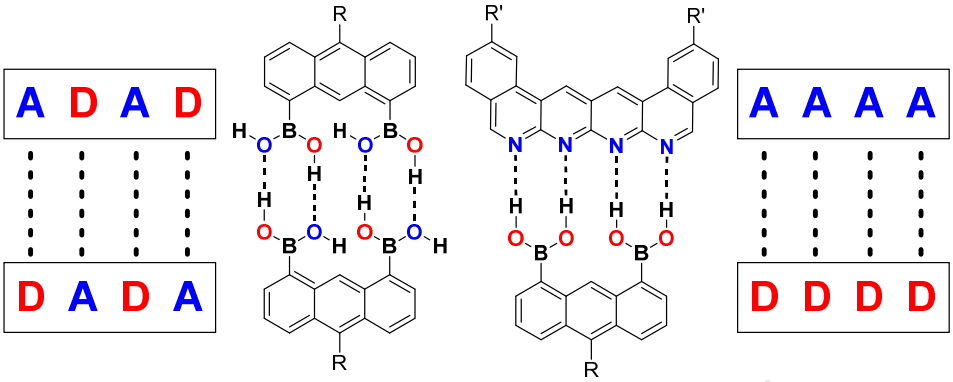

1,8,10-Trisubstituted anthracenyl hydrocarbons: towards versatile scaffolds for multiple-H-bonded recognition arrays.

Silvia Forensi,[1] Antoine Stopin,[2,3] Federica de Leo,[1] Johan Wouters,[1] Davide Bonifazi[2,3]*

[1]Dr. S. Forensi, Dr. F. de Leo, Prof. J. Wouters
Department of Chemistry, University of Namur, Rue de Bruxelles 61, 5000 Namur, Belgium

[2]Dr. A. Stopin, Prof. Dr. D. Bonifazi
School of Chemistry, Cardiff University, Main Building, Park Place, CF10 3AT, Cardiff, United Kingdom; E-mail: BonifaziD@cardiff.ac.uk

[3]Dr. A. Stopin, Prof. Dr. D. Bonifazi
Institute of Organic Chemistry, Faculty of Chemistry, University of Vienna, Währinger Str. 38, 1090, Vienna, Austria; E-mail: davide.bonifazi@univie.ac.at

Dedicated to Professor Nuno Maulide on the occasion of his receipt of the Tetrahedron Young Investigator Award.

Keywords: anthracene, polycyclic aromatic hydrocarbons, boronic acids, hydrogen-bonds

Abstract: In this work, we describe the synthesis of 1,8,10-trisubstituted anthracenyl scaffolds that, bearing boronic acid functionalities, can act as multiple H-bonding donor systems. The trisubstituted anthracenyl derivatives are synthesized following two main synthetic pathways. Whereas in the first approach trisubstituted anthracenyl derivatives are prepared through the regioselective addition of the relevant organomagnesium nucleophile to 1,8-dichloroanthraquinone, in the second avenue a triflate-bearing anthracene is prepared by reduction of the anthraquinone into the anthrone precursor and functionalized through metal-catalysed cross-coupling reactions. Complementary studies of the $Na_2S_2O_4$-mediated reduction of 1,8-dichloroanthraquinone allowed to shed further light on the possible mechanism of formation of the anthrone precursor, suggesting the presence of a *cis*-diol

intermediate undergoing antiperiplanar elimination. Solid-state X-ray diffraction investigations of the bisboronic acids show that the molecules self-assemble into dimers through the formation of four H-bonds established between the *anti-syn* conformers of the boronic acid moieties. ^{1}H-NMR titrations between bisboronic acids and tetra H-bond acceptor, diisoquinolino-naphthyridine, showed a significant shift of the -B(O*H*)$_2$ proton resonances, suggesting the presence of H-bonding interactions between both molecules.

1. Introduction

Organoboronic acids are one of the most important functional groups used in organic chemistry.[1] They are commonly used as organometallic species in Pd-catalysed Suzuki cross-coupling reactions,[2-5] in sensing,[6-9] and in dynamic covalent chemistry to form boronate esters.[10-13] In the recent years, organoboronic acids have also been proposed as versatile H-bonding donors.[14-19] Depending on the type of conformation adopted by the boronic acid functionality, i.e. *syn-syn*, *syn-anti* and *anti-anti*, they can form different non-covalent H-bonded arrays both in solution and in the solid state.[20] For instance, in the solid state phenylboronic acid undergoes formation of doubly-H-bonded dimers (DA-AD-type), in which the boronic acid moieties adopt a *syn-anti* conformation. The dimers are organised in tapes through the formation of lateral intermolecular H-bonds.[21,22] The same type of DA-AD interactions led to the formation of H-bonded polymers between phenylenediboronic acid whether the two moieties are located in the ortho,[23] meta[24] or para positions.[25] *Pedireddi et al.* also reported the formation of supramolecular assemblies of arylboronic acids with 4,4'-bipyridine.[26-28] Similarly, *Höpfl* and co-workers reported H-bonded polymers between 4,4'-bipyridine and different types of boronic acids.[29] More recently, *MacGillivray* and co-workers exploited the *syn-syn* conformer of boronic acid functionalities to organize 1,2-bis(4-pyridyl)ethylene in the solid state, and trigger a [2+2] photodimerization to yield *rctt*-tetrakis(4-pyridyl)cyclobutane stereoselectively (Figure 1).[30] Our group also reported the use of boronic acids to form doubly H-bonded complexes (DD-AA).[31] Cocrystallization of various arylboronic acids with either 1,8-naphtyridine or 5,6,11,12-tetraazanaphthacene yielded discrete H-bonded complexes, in which the boronic acid moiety are engaged in frontal H-bonding interactions through the *syn-syn* conformer (Figure 1). Notably, H-bonded polymers could be obtained with 1,4-diphenylboronic acid with 5,6,11,12-

tetraazanaphthacene.[31] However, to the best of our knowledge no examples of multiple H-bonded arrays involving boronic acids have been reported so far both in solution and in the solid state.

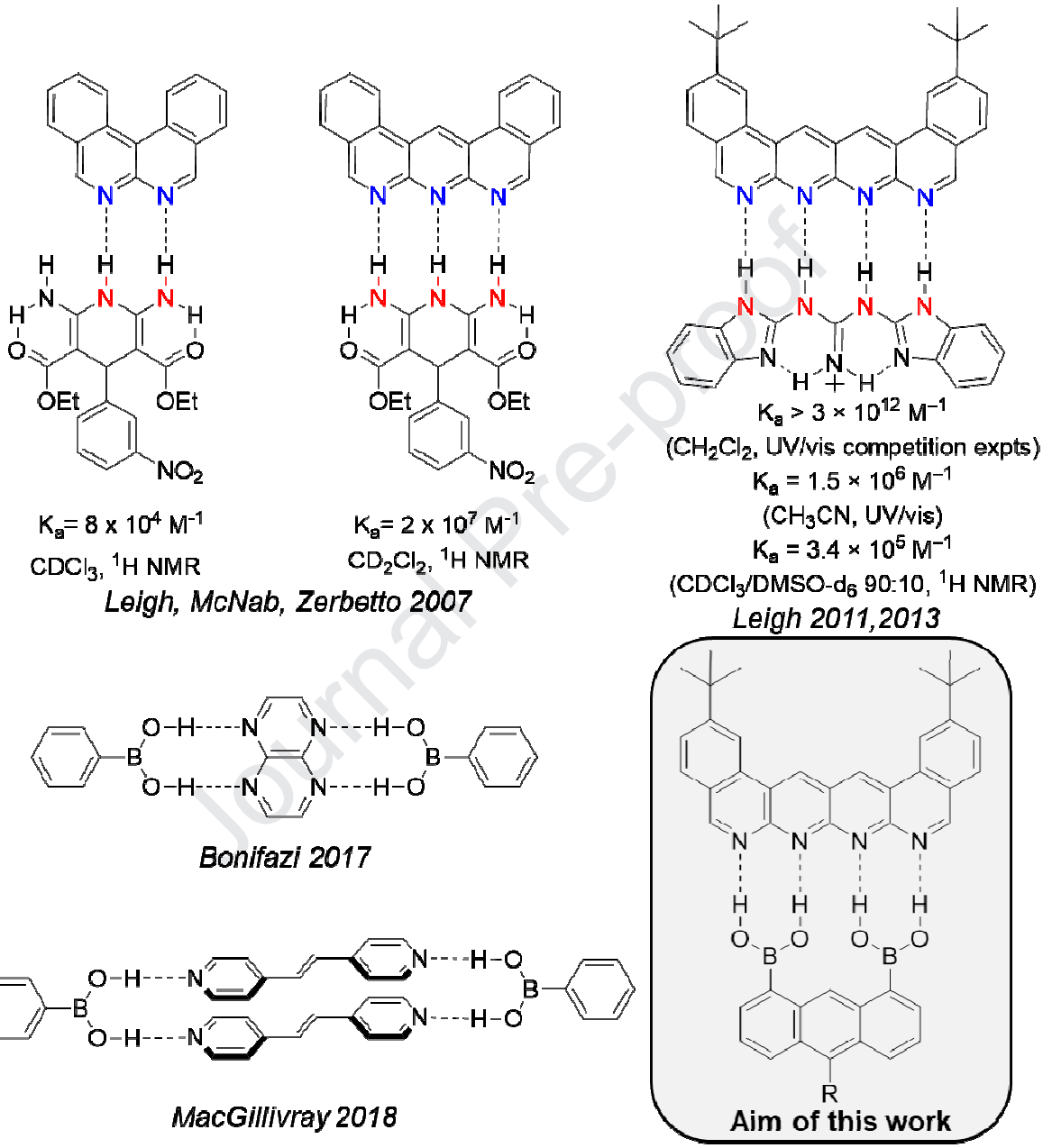

Figure 1. Common multiple H-bonded complexes[32-34,30,31] with (below) and without (above) boronic acids.

Due to their high directionality, selectivity, and reversibility, multiple *H*-bonding arrays are one of the most exploited non-covalent interactions for the preparation of self-assembled

functional organic architectures. In particular, linear *H*-bonded arrays have been extensively used to self-assemble and self-organise functional molecules into well-defined supramolecular architectures.[35-40] Through the demonstration with key examples in the field,[32,34,33] it has been shown that increasing the number of H-bonds in D-type arrays, the strength of association of is dramatically enhanced (Figure 1).[32,34,33] It is with this idea in mind that in this paper we describe our efforts to prepare suitable molecular structures that, bearing two boronic acid functionalities, could act as versatile scaffolds for preparing multiple H-bonded complexes. In particular, we have envisioned the preparation of *peri*-substituted anthracenyl derivatives that, bearing two frontal boronic acids at positions 1 and 8, could undergo formation of quadruple H-bonding interactions in the presence of a suitable acceptor (Figure 1).

2. Results and discussion

2.1 Design of the H-bonding systems: theoretical calculations

We began our investigation with the design of the boronic acid derivatives as H-bonding donors. Capitalizing on the DFT calculation, we modelled a substituted anthracenyl structure bearing boronic acids at *peri*-positions 1 and 8. Geometry optimization of the anthracenyl scaffolds was performed using DFT calculations at the B3LYP/6-311G** level of theory. In the optimized structure both boronic acid functionalities adopt a *syn-syn* conformation, arranging the acidic protons in a DDDD-type array. Notably, the non-acidic anthracenyl CH moiety in position 9 likely hampers the acid functionalities to be fully co-planar with the aromatic core (Figure 2a). When contacted to diisoquinolino-naphthyridine H-bond acceptor (AAAA), single point energy calculation showed that a highly stabilized quadrupole H-bonded complex (DDDD-AAAA) is formed with a predicted ΔH of -32.63 kcal/mol (Figure 2b). It is noteworthy to indicate that this value is superior to that reported for the formation of

doubly H-bonded dimers of phenylboronic acid with naphthyridine of -20.41 kcal/mol.[31] Encouraged by these predictive theoretical results, we planned the synthesis of the anthracenyl derivatives shown in Figure 2c. As we have anticipated limited solubility of bis-boronic acids in common organic solvents, anthracenyl cores bearing different substituents at position 10 have been prepared. The synthesis of H-bonding acceptor compound **1** (AAAA) was accomplished following a protocol reported in the literature (see also SI).[34]

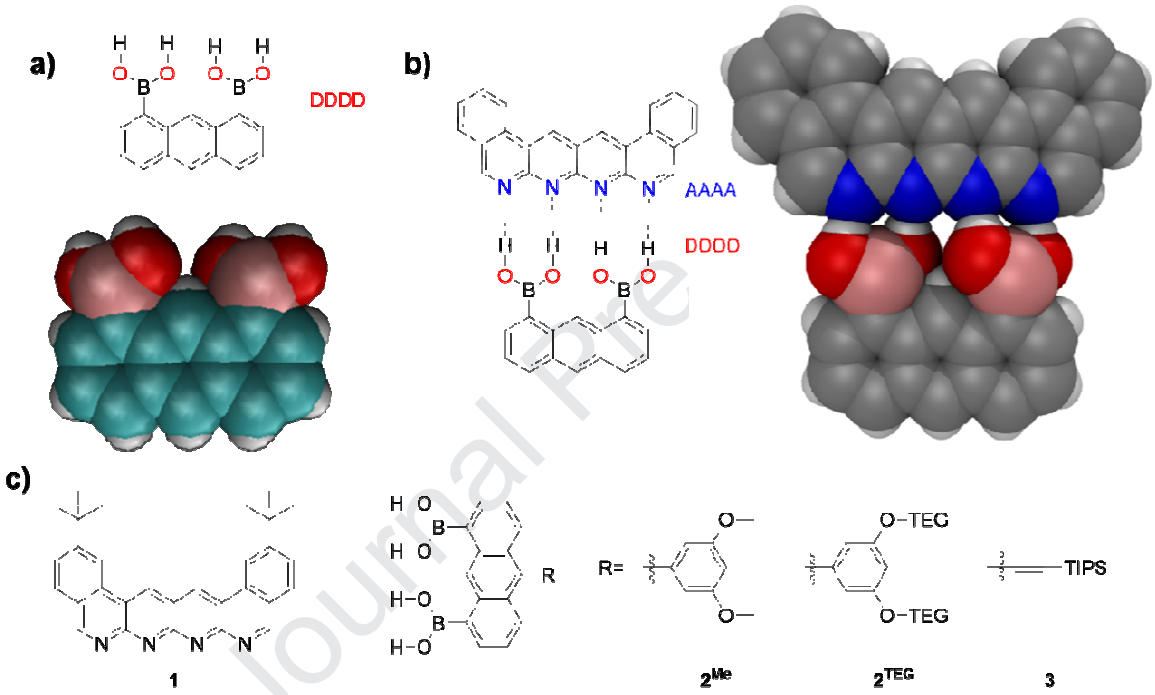

Figure 2. a) B3LYP optimized geometry of the donor backbone, **b)** B3LYP optimized geometry of the 4 H-bonded complex and **c)** structure of the target molecules.

2.2 Synthesis of three-substituted peri-functionalized anthracenyl scaffolds bearing H-bonding boronic acids.

Our investigations began with the synthesis of the H-bonding donor anthracenyl derivatives **2**^{Me}, **2**^{TEG}, and **3** each featuring a different solubilising group at position 10. Starting with compound **2**^{Me} (Scheme 1), bromo-derivative **4** was first reacted with Mg in THF to form its Grignard derivative that reacting with anthraquinone **5** at position 10, yielded hydroxyl-

bearing intermediate **6** in 67% yield. The structure of the addition product could be unambiguously determined by X-ray diffraction of single crystals obtained through evaporation of a solution of **6** in $CHCl_3$ (Figure 3a). As shown by the X-ray structure, molecule **6** adopts a puckered conformation, with the hydroxyl group H-bonded to a carbonyl group ($O_1\square\square\square O_2$ = 2.812(3) Å) of a neighbouring molecule in the crystal lattice. Halogen-halogen ($Cl_1\square\square\square Cl_2$ = 3.424(15) Å) and halogen-oxygen ($Cl_1\square\square\square O_2$ = 3.305(3) Å) short contacts were also observed. Reduction of ketone **6** with $LiAlH_4$ followed by addition of $BF_3{\cdot}Et_2O$ gave trisubstituted anthracenyl derivative $\mathbf{7^{Me}}$ in 95 % yield.

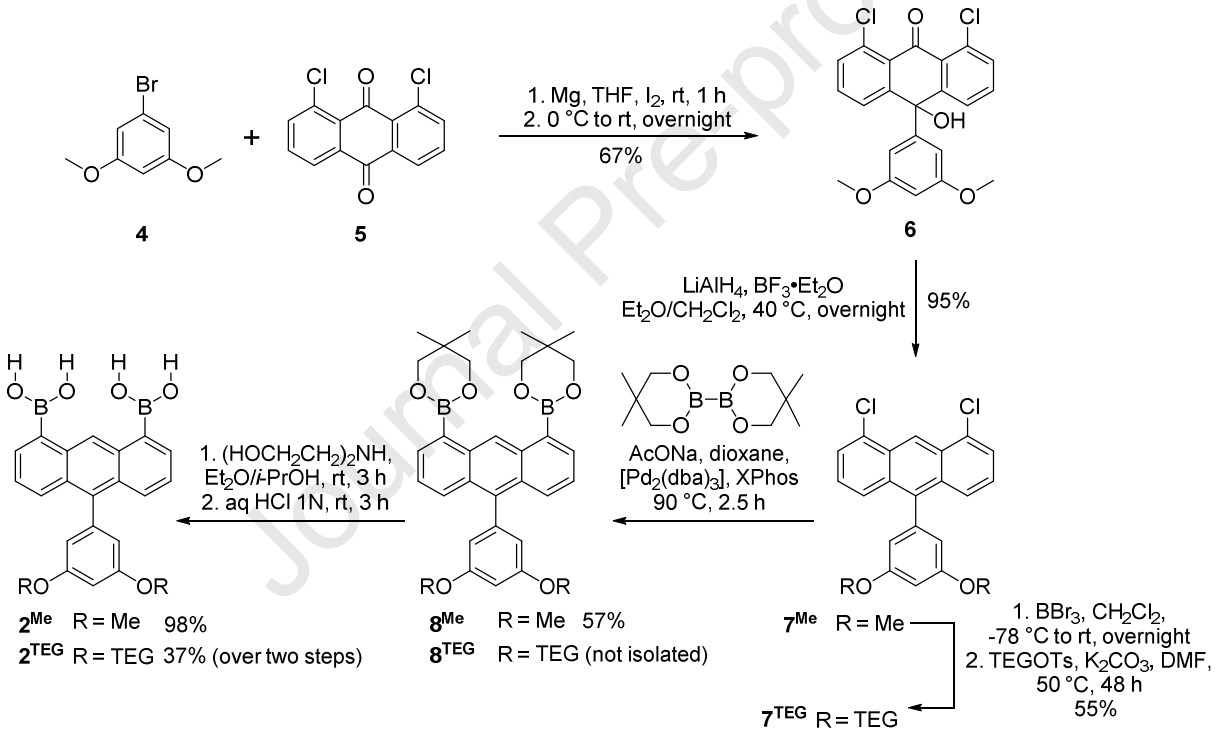

Scheme 1. Synthetic pathway to target anthracenyl derivatives $\mathbf{2^R}$.

Building on a literature protocol developed by *Tanaka*, *Wada* and co-workers, [41] *Miyaura* borylation of anthracene $\mathbf{7^{Me}}$ using bis(neopentylglycolato)diboron in the presence of NaOAc, $[Pd_2(dba)_3]$ and XPhos in 1,4-dioxane at 90 °C led to the formation of di-boronate ester $\mathbf{8^{Me}}$ in 57% yield. Transesterification with diethanolamine, followed by hydrolysis with HCl, led to

diboronic acid **2**^{Me} in 94% yield. Notably, molecule **2**^{Me} proved to be soluble only in DMSO. In addition to classical ^{1}H- and ^{13}C-NMR characterizations, the structures of the boronic acid derivative was confirmed by X-ray diffraction analysis of single crystals (for molecule **2**^{Me} see section 2.5). Suitable transparent crystals of diboronate **8**^{Me} for X-ray diffraction analysis were obtained from slow evaporation of a solution of $CHCl_3$ (Figure 3b). Pleasingly, the X-ray structure of compound **8**^{Me} shows that the two boronate ester moieties are fundamentally coplanar (dihedral angles O_1-B_1-C_1-C_6 = 17.6(5)° and O_2-B_1-C_1-C_2 = 16.7(5)°) with the anthracenyl scaffold. On the other hand, the aryl substituent is perpendicular to the polycyclic aromatic core (dihedral angle C_5-C_8-C_9-C_{10} = 88.5(4)°).

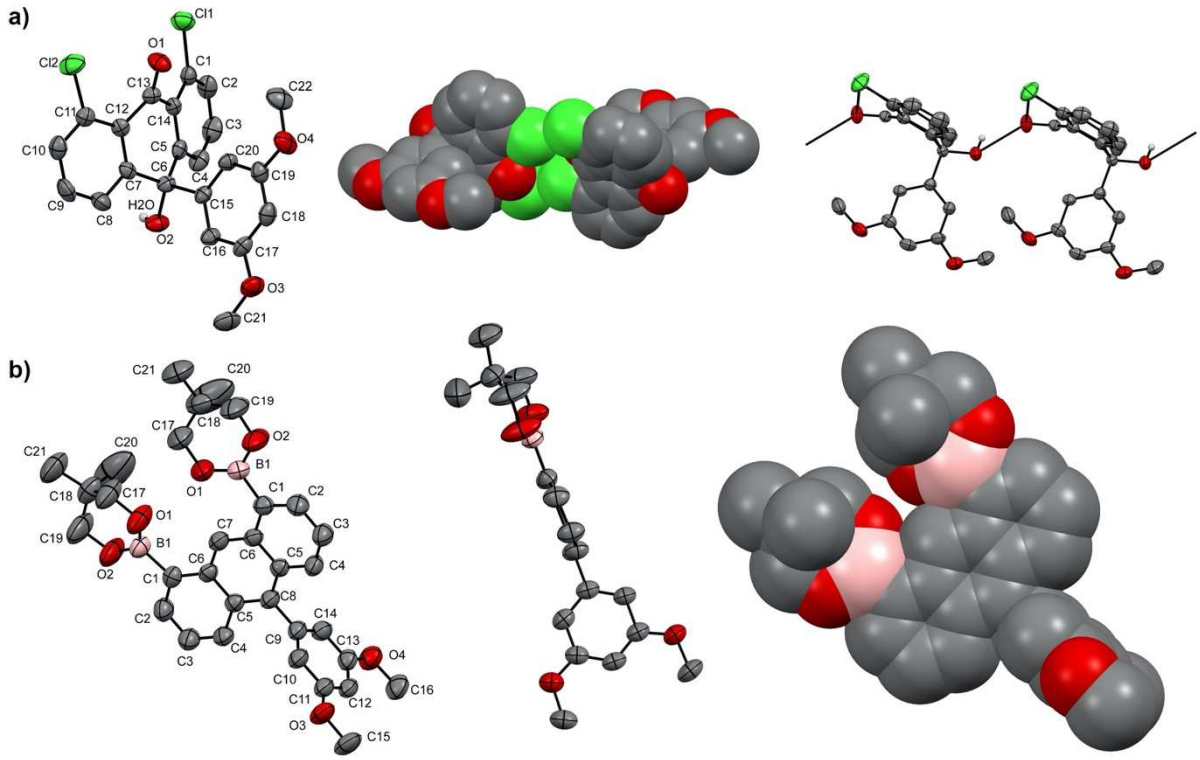

Figure 3. a) X-ray crystal structure of compound **6**; space group: P-2_1/n. **b)** X-ray crystal structure of compound **8**^{Me}; space group: Pnma. H atoms are omitted except for OH. Atom colours: green Cl, pink B, red O, grey C, white H

To improve the solubility of diboronic acid **2**^{Me} in organic solvents, molecular analogue **2**^{TEG} bearing two triethylene glycol tails was also prepared (Scheme 1**Error! Reference source**

not found.). In this case, demethylation of intermediate $\mathbf{7^{Me}}$ in the presence of BBr_3 in CH_2Cl_2 followed by alkylation with TEG-OTs under basic conditions led to compound $\mathbf{7^{TEG}}$ in 55% yield. Following the protocols (*i.e.*, *Miyaura* borylation and transesterification reactions followed by hydrolysis) described previously for installing the boronic acid moieties in molecule $\mathbf{2^{Me}}$, we prepared target molecule $\mathbf{2^{TEG}}$ in 37% yield over the two steps. Although the preparative route described so far led to the formation of the desired target molecules, this synthetic strategy is limited by the preparation of a suitable organometallic nucleophile. A more versatile synthetic approach would be one that allows the insertion of any substituents at position 10 through a metal-catalysed cross-coupling reaction. Indulging this line of thought, we turned our attention on anthracene derivative **9** (Scheme 2) as the key intermediate for the new route.

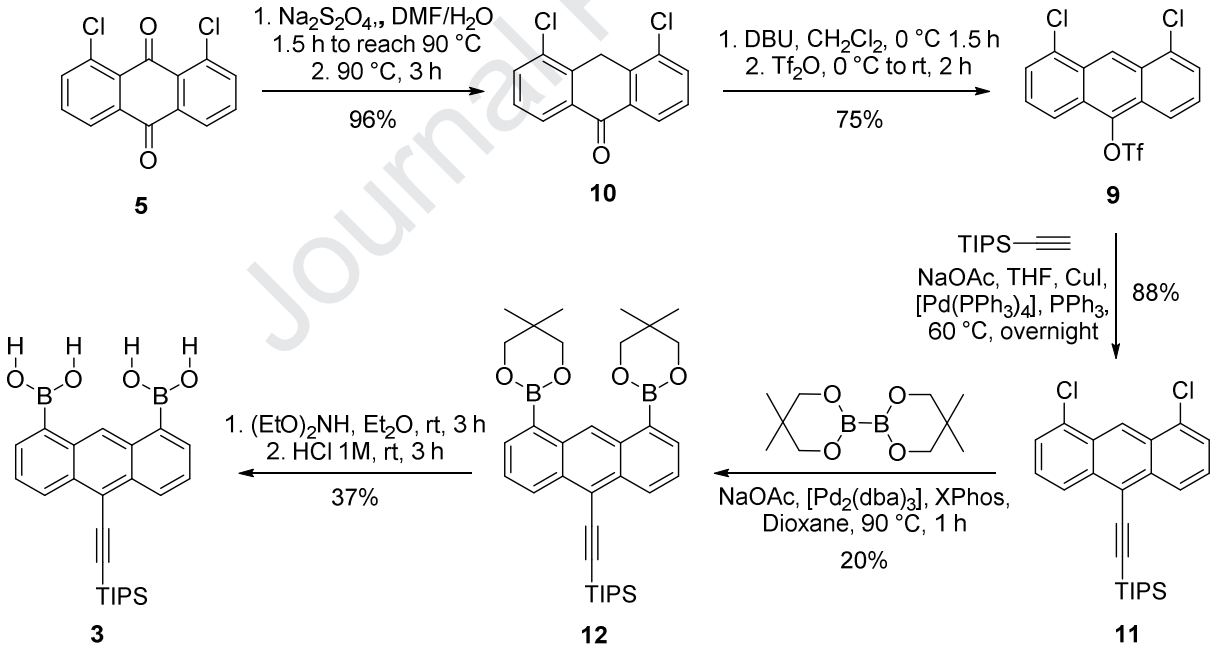

Scheme 2. Synthetic pathway to target molecule **3**.

The first synthetic step of this route involves the reduction of anthraquinone **5** to anthrone **10** with $Na_2S_2O_4$ (96% yield). The triflate insertion was obtained in 75% yield after

deprotonation of anthrone **10** with DBU followed by the addition of Tf_2O. The structure of anthracene **9** was confirmed by single crystal X-ray diffractions analysis (crystals obtained by slow evaporation of a $CHCl_3$ solution, Figure 4). The molecular packing is governed by the presence of π-π stacking as well as halogen-halogen interactions between chlorine and fluorine atoms. *Sonogashira*-type cross-coupling reaction between compound **9** and (triisopropylsilyl)acetylene (TIPSA) led to the formation of compound **11** in 88% yield. Following a similar protocol to that described previously for installing the boronic acid functionalities in molecules $\mathbf{2^R}$, target molecule **3** was obtained in moderate yield.

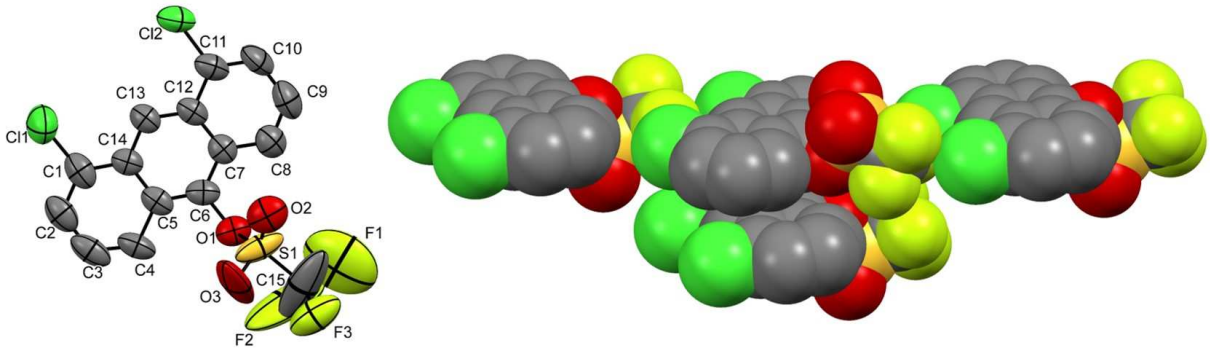

Figure 4. X-ray crystal structure of compound **9**; space group: C2/c. H atoms are omitted. Atom colours: green Cl, yellow S, pale green F, red O, grey C.

2.3 Study of the $Na_2S_2O_4$ reduction reaction of 1,8-dichloroanthraquinone.

While preparing the anthracenyl intermediates, the peculiar reduction conditions of 1,8-dichloroanthraquinone **5** with $Na_2S_2O_4$ stimulated our curiosity to shed further light on the mechanism of this reaction. In the literature, only a few studies address the challenge to unravel the mechanism of the $Na_2S_2O_4$-mediated reduction. In 1980 *Kellogg* and co-workers showed that, under basic conditions, $Na_2S_2O_4$ is an effective reagent for the reduction of aldehydes and ketones.[42] They suggested a two-step mechanism, in which an α-hydroxy sulfinate intermediate is formed followed by its reductive transformation with loss of SO_2. A

similar mechanism was also proposed the year after by *Saito* and co-workers.[43] In 1996, *Müller* and co-workers reported the regioselective reduction of *peri*-substituted anthraquinones into the relevant anthrones.[44] They hypothesised that the reduction undergoes formation of a diol intermediate that, in the presence of an acid, eliminates to give the relevant anthrone derivative. In a previous report, *Cristol* reported the rate of H_2O elimination from *cis*- and *trans*-9,10-anthraquinone diols. The author showed that the *syn* elimination, given by *trans* diols, is faster than that occurring with the *cis*-diols, with both diols being able to yield the relevant anthrone.[45] To commence, we prepared and isolated those reactive intermediates that, we think, are possibly lying on the reaction path to the anthrone product. In a first attempt, *peri*-substituted anthraquinone **5** was reacted with $Na_2S_2O_4$ at room temperature for 5 h (Scheme 3). Interestingly, under these reaction conditions intermediate 9-hydroxy-10-anthrone **13** was quantitatively obtained (structure confirmed by X-Ray diffraction analysis of crystals obtained through vapor diffusion of cyclohexane into a CH_2Cl_2 solution, Figure 5a).

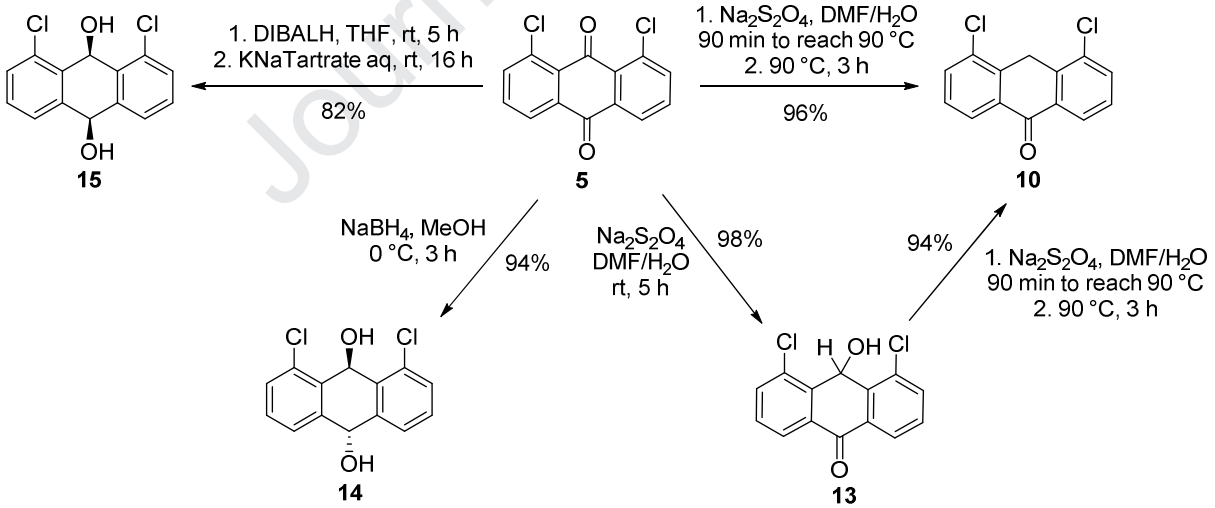

Scheme 3. Mechanistic study of the $Na_2S_2O_4$-mediated reduction of 1,8-dichloroanthraquinone to anthrone **10**: synthesis of the envisaged intermediates.

Successive reaction of **13** with $Na_2S_2O_4$ at 90 °C led to anthrone **10** in 94% yield, the structure of which could also be confirmed by X-ray diffraction (Figure 5b). These observations

suggested that the $Na_2S_2O_4$-mediated reduction could occur stepwise, with the formation of 9-hydroxy-10-anthrone in the first place, and of a diol anthraquinone in the later stage. To confirm this hypothesis, both *cis*- and *trans*- diols of 1,8-dichloroanthraquinone were also synthesized (Scheme 3). *trans*-Diol **14** was obtained by reaction of **10** in the presence of $NaBH_4$ in MeOH at 0 °C for 3 h, whereas *cis*-diol analogue **15** could be prepared in 82% yield using DIBALH in THF.

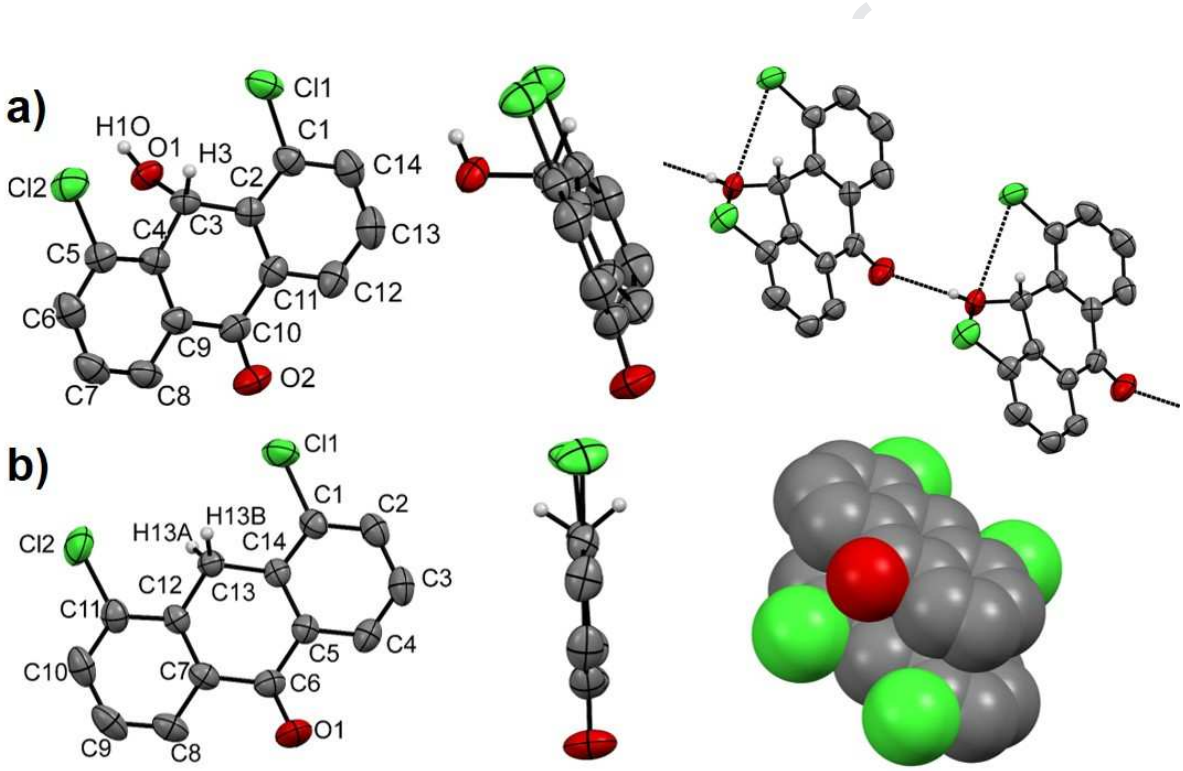

Figure 5. a) Crystal structure of compound **13**; space group: $P2_1/c$. **b)** Crystal structure of compound **10**; space group: $P\text{-}2_1$. H atoms are omitted except for OH and Csp_2H. Atom colours: green Cl, red O, grey C, white H.

The conformational properties of both 1,8-dichloroanthraquinone diols were confirmed by single-crystal X-Ray diffraction analyses. The structures of both diols were determined from crystals obtained by slow evaporation of acetone solutions (Figure 6a). Interestingly, molecules of *trans*-diol **14** arrange in a tape-like network through H-bonding interactions, connecting four neighbouring molecules ($O_1\square\square\square O_2$ = 2.867(4) Å and $O_1\square\square\square O_2$ = 2.926(4)

Å). In this isomer, the two hydroxyl groups are in equatorial and axial positions, respectively. On the other hand, the X-ray structure of *cis*-diol **15** shows the presence of the two hydroxyl groups in axial positions (Figure 6b) linked through an intramolecular H-bond ($O_1\square\square\square O_2$ = 2.876(3) Å). The molecules organise into dimers held together by two, squarely arranged H-bonds ($O_1\square\square\square O_2$ = 2.921(3) Å). *trans*- and *cis*-Diols **14** and **15** were used to unravel the possible elimination pathways leading to anthrone **10**.

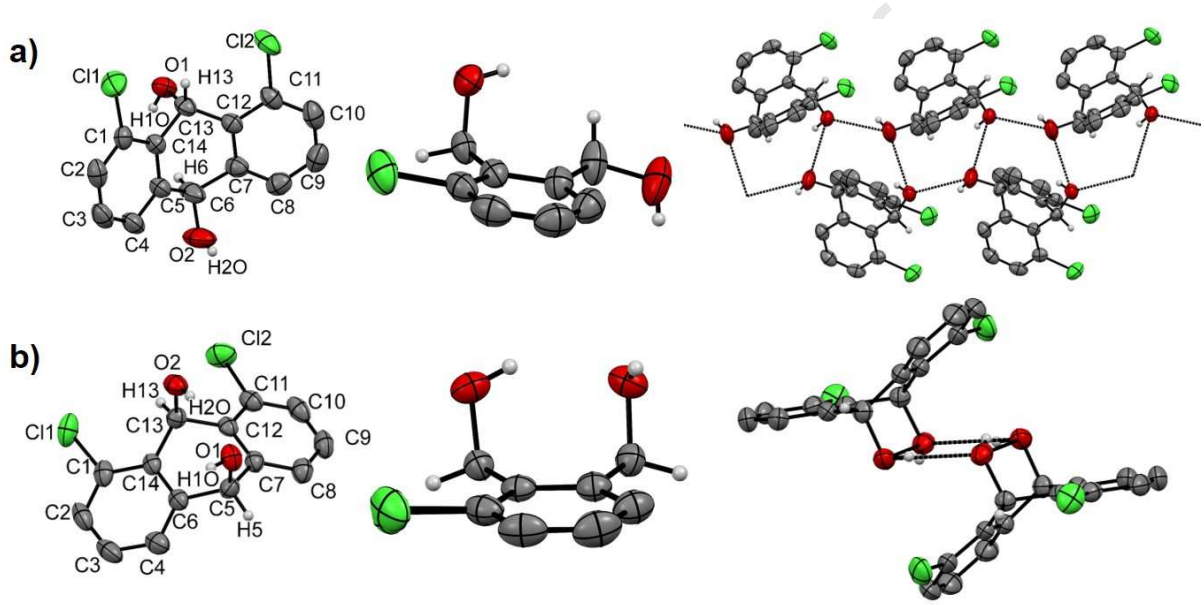

Figure 6. a) Crystal structure of compound **14**; space group: $P2_1$. **b)** Crystal structure of compound **15**; space group: P-1. H atoms are omitted except for OH and Csp_2H. Atom colours: green Cl, red O, grey C, white H.

As the first experiment, the thermal elimination in DMF/H_2O at 90 °C for 5 h was attempted with *trans*- and *cis*-diols **14** and **15** (Table 1, entries 1&2). In both cases, no conversion was observed, which clearly suggest that heat alone is not sufficient for the reaction to occur. Therefore, we reacted independently *trans*- and *cis*-diols **14** and **15** in the presence of $Na_2S_2O_4$ at 90 °C for 5 h following the protocol conditions used to transform 1,8-dichloroanthraquinone **5** into anthrone **10**. Whereas *trans*-diol **14** did not yield any product, the reaction with *cis*-diol **15** led to the formation of anthrone **10** in 64% yield (Table 1, entries

3&4). This observation suggests that *cis*-diol **15** is likely the intermediate that, formed in the $Na_2S_2O_4$-mediated reduction, allows the transformation of quinone **5** into anthrone **10**. When the diols are reacted independently in the presence of HCl at 90 °C for 5 h, both led to desired anthrone **10** quantitatively (Table 1, entries 5&6), as previously suggested by *Cristol*.

Table 1. Mechanistic study of the $Na_2S_2O_4$-mediated reduction of 1,8-dichloroanthraquinone to anthrone **10**: reduction attempts of diols **14** (*trans*) and **15** (*cis*).

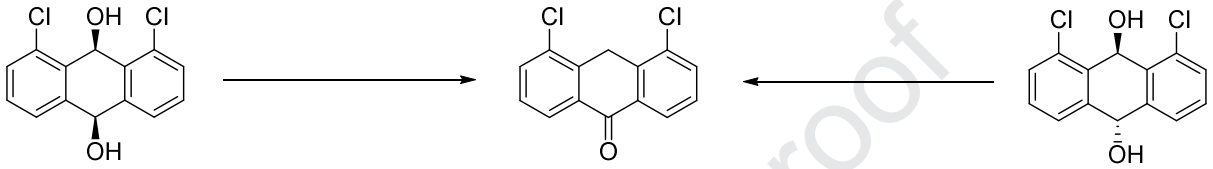

entry	Diol	Reagent	Solvent	Time	Temperature	Yield
1	**14**	-	DMF/H_2O	5 h	90 °C	0%
2	**15**	-	DMF/H_2O	5 h	90 °C	0%
3	**14**	$Na_2S_2O_4$	DMF/H_2O	5 h	90 °C	0%
4	**15**	$Na_2S_2O_4$	DMF/H_2O	5 h	90 °C	64%
5	**14**	HCl	DMF/H_2O	5 h	90 °C	96%
6	**15**	HCl	DMF/H_2O	5 h	90 °C	93%

Taken all together, these observations suggest that the $Na_2S_2O_4$-mediated reaction to anthrone **10** follows an antiperiplanar elimination pathway as only the *cis* isomer reacts under these reductive conditions (Scheme 4). Indeed, only *cis*-diol **15** can adopt a conformation suitable for an antiperiplanar elimination, i.e. hydrogen atom and hydroxyl group in *axial* positions. The elimination can occur through two different routes (Scheme 5). In route 1, a HSO_3^- anion, generated from thermal decomposition of $Na_2S_2O_4$, may deprotonate the axial hydrogen triggering an E_{1cb}-type elimination reaction (top, Scheme 5). In route 2, an antiperiplanar E_2-like elimination is proposed (down, Scheme 5). In both mechanistic propositions, a sulfinate

moiety is evoked as leaving group (possibly formed in the presence of $Na_2S_2O_4$ under refluxing conditions).

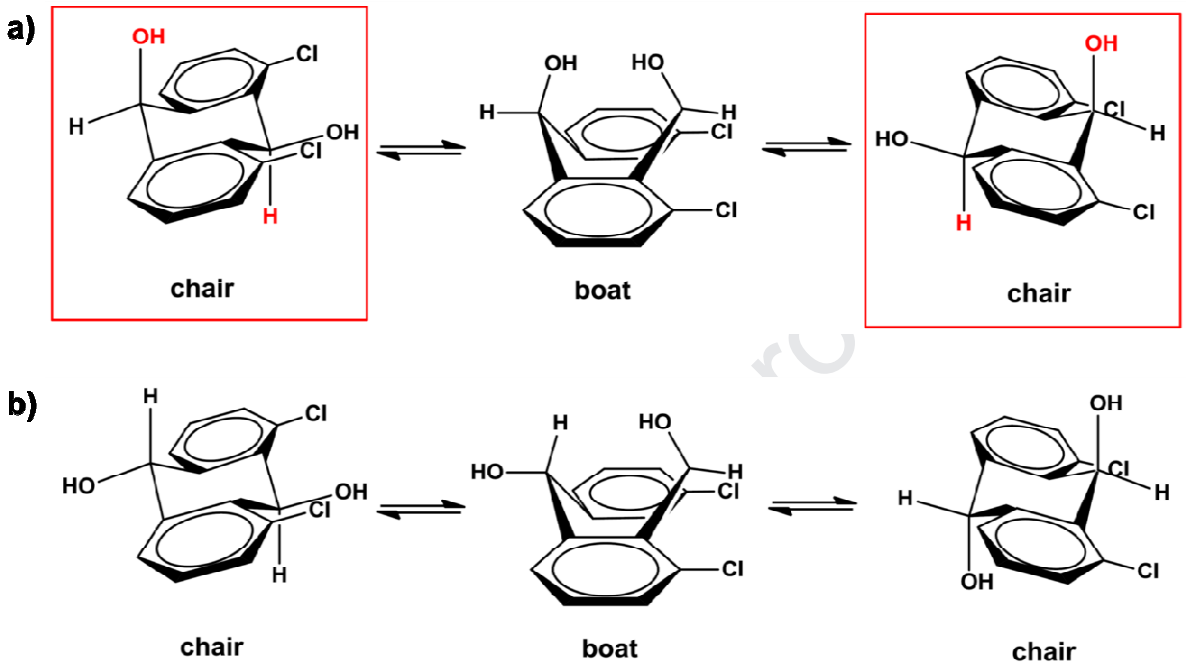

Scheme 4. Possible conformations of **a)** *cis*-diol **15** and **b)** *trans*-diol **14**. The red squares indicate the only conformation able to give antiperiplanar elimination.

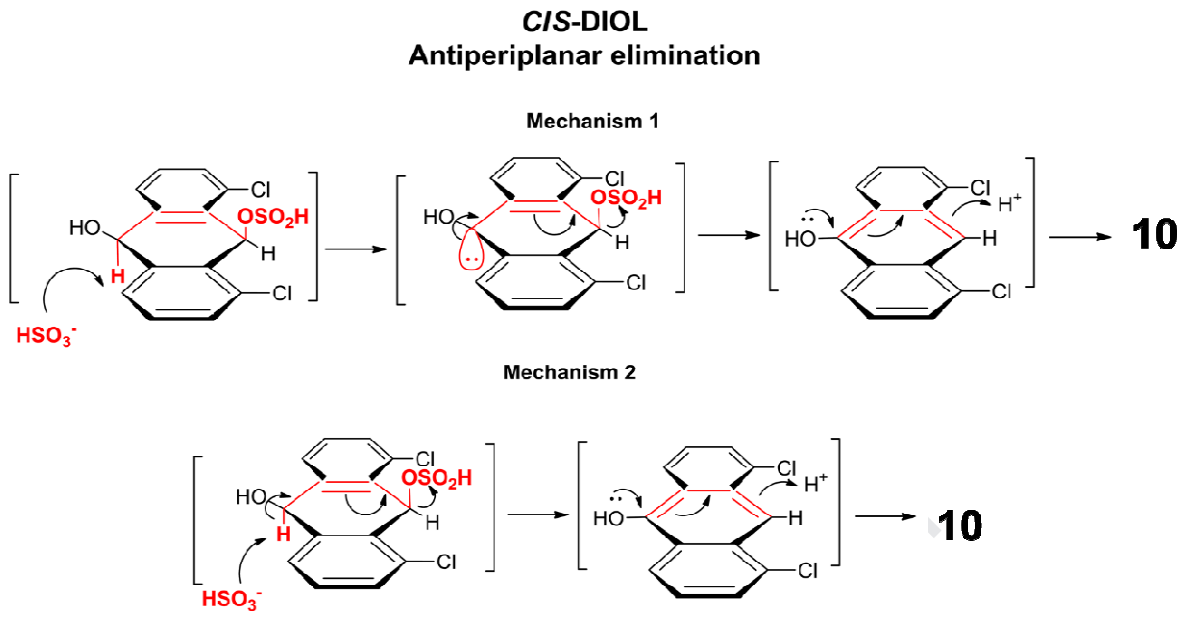

Scheme 5. Possible antiperiplanar elimination routes.

2.4 Homomolecular and heteromolecular hydrogen-bonding recognition properties.

2.4.1 H-bonding recognition at the solid state.

Suitable crystals of $\mathbf{2^{Me}}$ for X-ray diffraction analysis were obtained by vapor diffusion of H_2O into a DMSO solution (Figure 7a). In the solid state, molecule $\mathbf{2^{Me}}$ dimerizes into H-bonded complexes ($\mathbf{2^{Me}}$•$\mathbf{2^{Me}}$), in which each boronic acid moiety frontally engages into double DA-AD-type arrays (O_1□□□O_4 = 2.850(3) Å and O_2□□□O_3 = 2.787(3) Å) as *syn-anti* conformers.

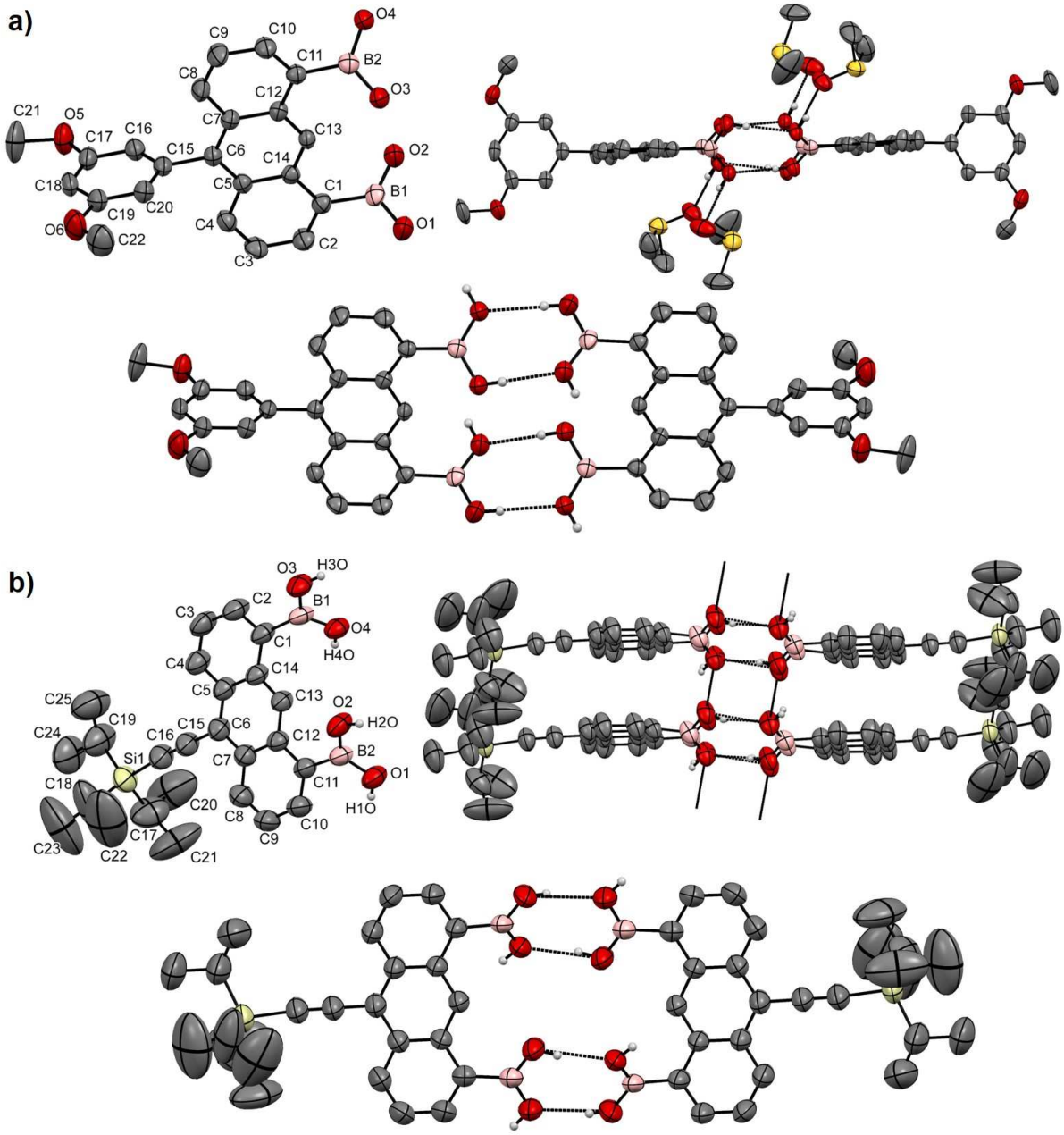

Figure 7. a) X-ray crystal structure of compound $\mathbf{2^{Me}}$; space group: P-2_1/c. **b)** X-ray crystal structure of compound **3**; space group: C2/c. H atoms are omitted except for $B(OH)_2$. Atom colours: pink B, red O, pale yellow Si, yellow S, grey C, white H.

Notably, the *syn-anti* conformational preference of the hydroxyl groups forces the boronic acid moieties in the *peri*-positions to twist, and adopt a non-planar arrangement with the anthracene core (dihedral angles: O_1-B_1-C_1-C_2 = 58.9(3)°, O_2-B_1-C_1-C_{14} = 59.2(3)°, O_3-B_2-C_{11}-C_{12} = 38.1(4)° and O_4-B_2-C_{11}-C_{10} = 36.5(5)°). The arrangement of the boronic acids

observed in $\mathbf{2^{Me}}$ contrasts that observed for the boronate ester moieties in compound $\mathbf{8^{Me}}$, in which the boron-containing functionalities and the polycyclic aromatic skeleton are co-planar. Solvent molecules of DMSO are also present in the crystal, each H-bonded with the hydroxyl moieties of $\mathbf{2^{Me}}$ ($O_2\square\square\square O_8$ = 2.638(16) Å and $O_4\square\square\square O_7$ = 2.650(3) Å). Suitable crystals of molecule **3** were obtained by vapor diffusion of EtOH into a $CHCl_3$ solution (Figure 7b). As for molecule $\mathbf{2^{Me}}$, derivative **3** dimerizes into H-bonded complexes (**3●3**), in which each boronic acid moiety adopts a *syn-anti* conformation and frontally engages into double DA-AD-type H-bonding arrays ($O_1\square\square\square O_3$ = 2.781(3) Å and $O_2\square\square\square O_4$ = 2.787(4) Å). In contrast to the crystal packing of molecule $\mathbf{2^{Me}}$, each complex **3●3** establishes lateral H-bonds with adjacent dimers ($O_1\square\square\square O_3$ = 2.798(3) Å) forming a ladder-type network. As for $\mathbf{2^{Me}}$●$\mathbf{2^{Me}}$, the boronic acid moieties and the anthracenyl core adopt a non-planar conformation in dimer **3●3**.

2.4.2 Heteromolecular H-bonding recognition in solution.

At last, we attempted to study the formation of H-bonded heteromolecular complexes in solution using boronic acids derivatives ($\mathbf{2^{R}}$ and **3**) as the H-bonding DDDD partners and molecule **1** as the complementary AAAA-type acceptor. Due to the poor solubility of boronic acids $\mathbf{2^{Me}}$ and **3** in non-competitive organic solvents, any attempts to study their H-bonding recognition properties by ^{1}H-NMR titration failed. Thus we turned out attention to UV-vis absorption spectroscopy, and monitored any changes in the absorption profile of H-bonding acceptor **1** (c = 10^{-6} mol L^{-1} in CH_2Cl_2) upon increasing amount of H-bonding donor $\mathbf{2^{Me}}$ (Figure 8). As one can clearly notice in the absorption profiles shown in Figure 8, only a decrease in the intensity of the absorption bands characteristic of acceptor **1** (420 to 470 nm) was observed upon increasing addition (up to 0.5 equivalents) of donor $\mathbf{2^{Me}}$. No energy shifts

were observed for any of the electronic transitions. Further increases of the concentration of $\mathbf{2}^{\mathbf{Me}}$ (up to 3 equivalents) did not lead to any significant changes of the absorption envelop of acceptor **1**. If one considers that shifts in energy are frequently observed for the strongest absorption bands when a chromophore engages in H-bonding interactions in solution, we concluded that if a non-covalent complex is formed, this crashes out of solution (some precipitate was observed in the cuvette). H-bonding donor **3** displayed a similar behaviour to that of $\mathbf{2}^{\mathbf{Me}}$, whereas no spectral changes were observed when $\mathbf{2}^{\mathbf{TEG}}$ was used. Despite the numerous attempts, we could not grow suitable crystals for X-ray diffraction analysis of the H-bonded complexes ($\mathbf{2}^{\mathbf{Me}}\bullet\mathbf{1}$ and $\mathbf{3}\bullet\mathbf{1}$).

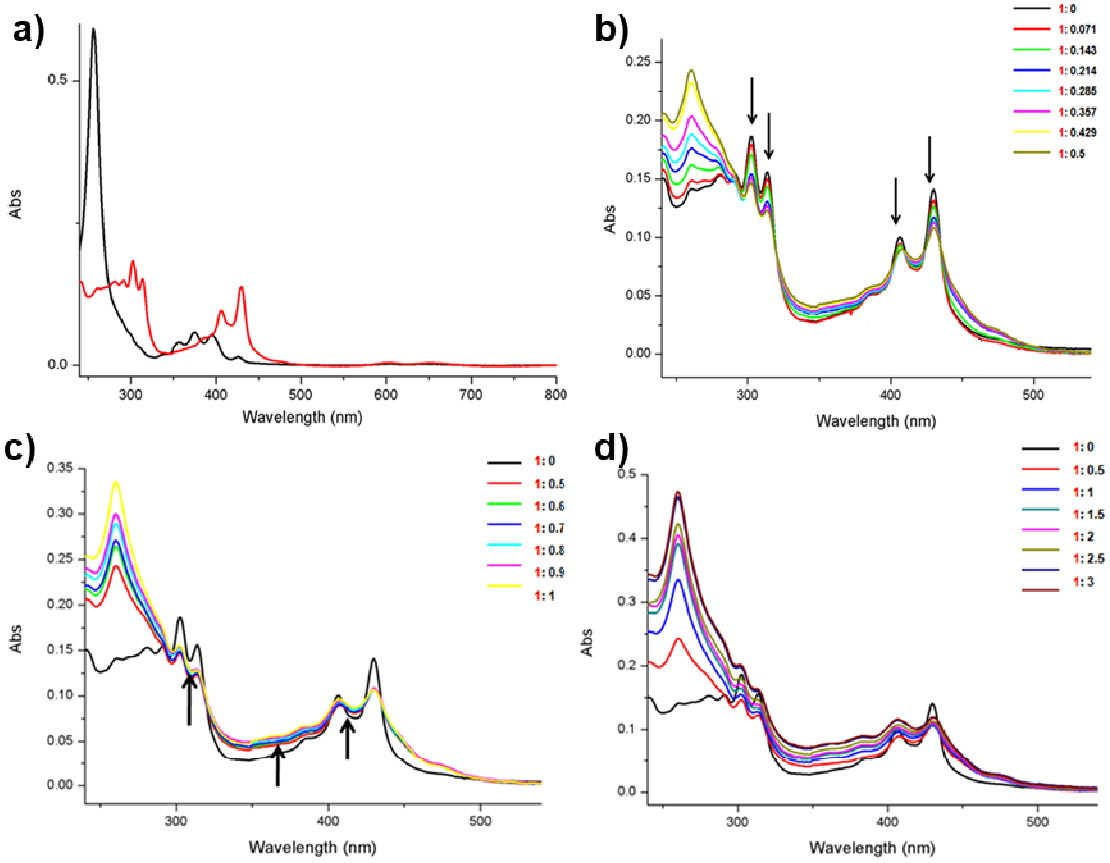

Figure 8. a) UV-vis absorption profiles of acceptor **1** (red) and donor $\mathbf{2^{Me}}$ (black) in CH_2Cl_2 at 10^{-6} M. **b)-d)** UV-Vis titration experiments in CH_2Cl_2 of acceptor **1** (10^{-6} M) with donor $\mathbf{2^{Me}}$ (the **1**:$\mathbf{2^{Me}}$ ratio is displayed in the legend).

Given the good solubility of H-bonding donor $\mathbf{2^{TEG}}$ in organic solvents, we studied the binding of $\mathbf{2^{TEG}}$ with **1** by means of ^{1}H-NMR titration. As peaks fingerprinting the boronic acid protons are generally not visible in $CDCl_3$,[31] a 1:1 mixture of C_6D_6 and THF-d_8 was first employed, but extensive precipitation occurred upon addition of both components to the solution. Instead, reduced precipitation was noticed with a 95:5 mixture of C_6D_6 and DMSO-d_6. Titration experiments were thus performed in the latter solvent mixture using H-bonding donor $\mathbf{2^{TEG}}$ and acceptor **1** as host and acceptor**,** respectively.

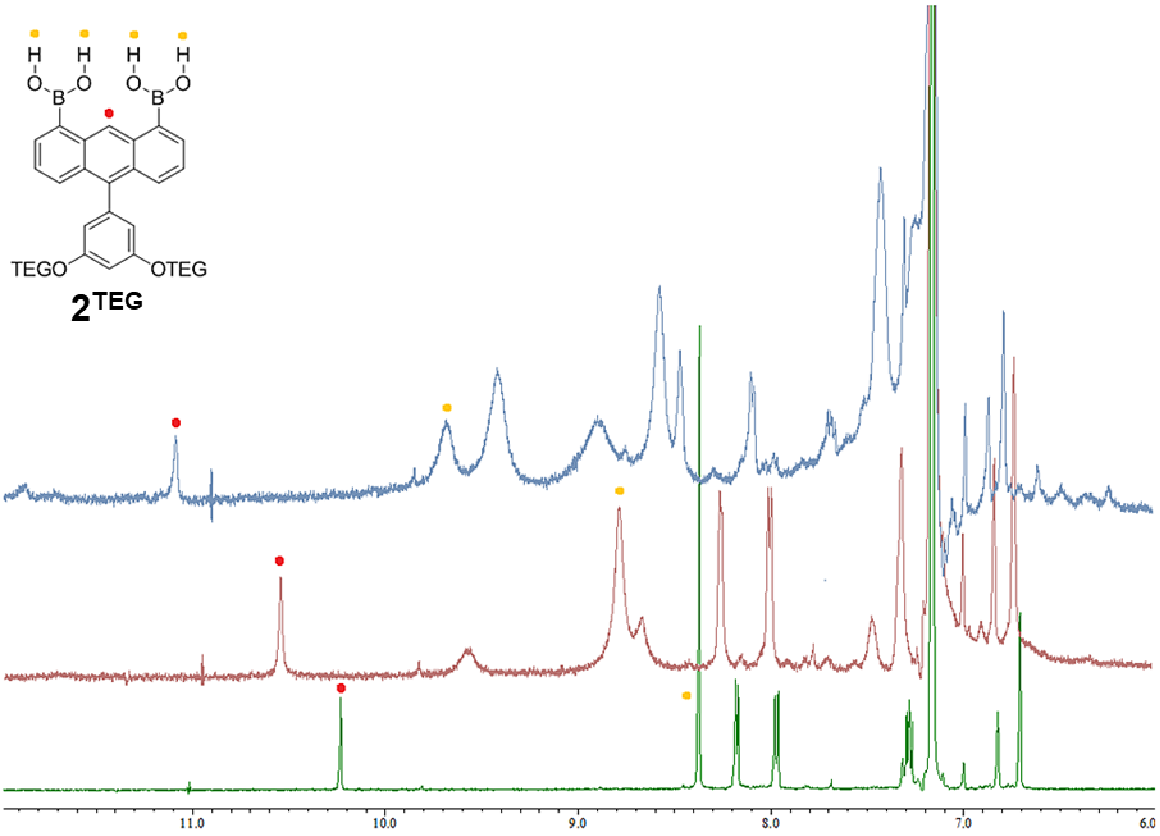

Figure 9. Selected regions of ^{1}H NMR titration experiments of H-bonding donor $\mathbf{2}^{\mathbf{TEG}}$ (5 mM) upon addition of H-bonding acceptor **1** (500 MHz, C_6D_6/DMSO-d_6 95/5, 298 K). The dots indicate the diagnostic proton resonances of H-bonding donor $\mathbf{2}^{\mathbf{TEG}}$. The molar ratios $\mathbf{2}^{\mathbf{TEG}}$:**1** of the different spectra are: 1:0 (bottom), 1:0.5 (middle), 1:1 (top).

Although some precipitation and peak broadening were observed during the titration experiments (Figure 9), addition of increasing amount of **1** to a 5 mM solution of $\mathbf{2}^{\mathbf{TEG}}$ led to noticeable downfield shift ($\Delta\delta = 1.31$ ppm) of the -B(O*H*)$_2$ proton resonances, suggesting the presence of H-bonding interactions. Together with the-B(O*H*)$_2$ resonances, also the peaks of the proton resonance of the aromatic *peri*-proton CH in position 9 revealed significant downfield shifts ($\Delta\delta = 0.49$ ppm) upon addition of **1**, confirming the presence of interactions involving the frontal boronic acid moieties. Unfortunately, the slight precipitation observed during the titration experiments together with the significant peak broadening (Figure 9) hampered any further attempts to produce meaningful thermodynamic data in solution.

3. Conclusion

In summary, herein we developed two synthetic pathways to prepare 1,8,10-trisubstituted anthracenes that, bearing two boronic acid functionalities, can act as multiple H-bonding donors. Whereas in the first approach the *peri*-substituted anthracenyl derivatives are synthesized through the addition of a Grignard nucleophile to 1,8-dichloroanthraquinone, in the second avenue a triflate-bearing 1,8,10-trisubstituted anthracene is prepared by $Na_2S_2O_4$ reduction of the anthraquinone into the anthrone precursor and functionalized through a metal-catalysed cross-coupling reaction. Complementary studies of the $Na_2S_2O_4$-mediated reduction of 1,8-dichloroanthraquinone allowed to shed further light on the mechanism leading to the anthrone intermediate, suggesting that the reaction possibly involves the formation of a *cis*-diol derivative that can undergo antiperiplanar elimination. X-ray diffraction investigations of the 1,8,10-trisubstituted anthracenyl boronic acids in the solid-state show that the molecules self-assemble into dimers through the formation of frontal H-bonds established between the *anti-syn* conformers of the boronic acid moieties. The binding properties of the boronic acids (DDDD) were also studied in solution in the presence of a suitable multiple H-bonding acceptor (AAAA), diisoquinolino[3,4-b:4',3'-g][1,8]naphthyridine. While UV-Vis spectroscopic investigations did not lead to any conclusive observations, ^{1}H-NMR titration experiments showed a significant downfield shift of the -B(O*H*)$_2$ proton resonances, suggesting the presence of H-bonding interactions. However, the poor solubility of the H-bonded complexes hampered precise determination of the stoichiometry of the complexes and of any thermodynamic parameters.

4. Experimental part

General Methods

Chemicals were purchased from *Sigma Aldrich, Acros Organics, Fluorochem, TCI, Carbosynth,* and *ABCR,* and were used as received. Solvents were purchased from *Sigma Aldrich* and *Acros Organics*. Deuterated solvents were purchased from *Eurisotop*. General solvents were distilled *in vacuo*. Anhydrous solvents such as Et_2O and THF were distilled from Na/benzophenone; CH_2Cl_2 from phosphorus pentoxide. Anhydrous DMF, 1,4-dioxane and MeOH were purchased and used without further purification. Anhydrous conditions were achieved by drying *Schlenk* lines, 2-neck flasks or 3-neck flasks by flaming with a heat gun under vacuum and purging with argon. The inert atmosphere was maintained using argon-filled balloons equipped with a syringe and needle that was used to penetrate the silicon stoppers used to close the flasks' necks. The addition of liquid reagents was done by means of dried plastic syringes or by cannulation. **Column chromatography** was carried out using *Grace* silica gel 60 (particle size 40-63 μm). **Melting points** (m.p.) were measured on a *Büchi Melting Point B-545*. All of the melting points have been measured in open capillary tubes and have not been corrected. **Nuclear magnetic resonance** (NMR) ^{1}H and ^{13}C spectra were obtained on a 400 MHz NMR *(Jeol JNM EX-400).* Chemical shifts were reported in ppm according to tetramethylsilane using the solvent residual signal as an internal reference ($CDCl_3$: ^{1}H = 7.26 ppm, ^{13}C = 77.16 ppm, CD_2Cl_2: ^{1}H = 5.32 ppm, ^{13}C = 53.84 ppm, CD_3OD: ^{1}H = 3.10 ppm, ^{13}C = 49.00 ppm, DMSO-d_6: ^{1}H = 2.50 ppm, ^{13}C = 39.52 ppm, $(CD_3)_2CO$: ^{1}H = 2.05 ppm, ^{13}C = 29.84 ppm). Coupling constants (*J*) were given in Hz. Resonance multiplicity was described as *s* (singlet), *d* (doublet), *t* (triplet), *q* (quartet). Carbon spectra were acquired with a complete decoupling for the proton. All spectra were recorded at 25 °C. **Infrared spectra** (IR) were recorded on a *Perkin-Elmer Spectrum II FT-IR System UATR*, mounted with a diamond crystal. Selected absorption bands are reported in wavenumber (cm^{-}

[1]). **Mass spectrometry** was generally performed by the *Fédération de Recherche ICOA/CBM (FR2708) platform* of Orléans in France. High-resolution ESI mass spectra (HRMS) were performed on a *Bruker maXis Q-TOF* in the positive ion mode. The analytes were dissolved in a suitable solvent at a concentration of 1 mg/mL and diluted 200 times in methanol (≈ 5 ng/mL). The diluted solutions (1μL) were delivered to the ESI source by a *Dionex Ultimate 3000 RSLC* chain used in FIA (Flow Injection Analysis) mode at a flow rate of 200 μL/min with a mixture of CH_3CN/H_2O + 0.1% of HCO_2H (65/35). ESI conditions were as follows: capillary voltage was set at 4.5 kV; dry nitrogen was used as nebulizing gas at 0.6 bars and as drying gas set at 200 °C and 7.0 L/min. ESI-MS spectra were recorded at 1 Hz in the range of 50-3000 *m/z*. Calibration was performed with ESI-TOF Tuning mix from Agilent and corrected using lock masses at *m/z* 299.294457 (methyl stearate) and 1221.990638 (HP-1221). Data were processed using *Bruker DataAnalysis 4.1* software. MALDI-MS were performed by the *Centre de spectrométrie de masse* at the *Université de Mons* and recorded using a *Waters QToF Premier* mass spectrometer equipped with a nitrogen laser, operating at 337 nm with a maximum output of 500 mW delivered to the sample in 4 ns pulses at 20 Hz repeating rate. Time-of-flight mass analyses were performed in the reflectron mode at a resolution of about 10,000. The matrix solution (1 μL) was applied to a stainless-steel target and air dried. Analyte samples were dissolved in a suitable solvent to obtain 1 mg/ml solutions. 1 μL aliquots of those solutions were applied onto the target area already bearing the matrix crystals, and air dried. For the recording of the single-stage MS spectra, the quadrupole (rf-only mode) was set to pass ions from 100 to 1000 Th, and all ions were transmitted into the pusher region of the time-of-flight analyser where they were analyzed with 1 s integration time.

10-(3,5-dimethoxyphenyl)anthracene-1,8-diyl)diboronic acid 2^{Me}

To a suspension of compound **8^{Me}** (100 mg, 0.186 mmol) in Et_2O (9.6 mL), a solution of diethanolamine (40 µL, 0.409 mmol) in *i*-PrOH (2 mL) was added. The mixture was stirred for 3 h at room temperature and the solution filtered. The solid was suspended in 1M *aq* HCl (6.4 mL). The mixture was stirred at room temperature for 3 h, filtered and the solid washed with H_2O (3×5 mL). The solid was dried using a freeze-dryer overnight to yield compound **2^{Me}** (73 mg, 98%) as a bright yellow powder. M.p. 276-277°C. FTIR (ATR) ν (cm^{-1}): ν 3375, 1590, 1381, 1201, 1150, 1061, 1030, 992, 755, 739. ^{1}H-NMR (400 MHz, DMSO-d_6): δ 9.43 (s, 1H), 8.35 (s, 4H), 7.64 (d, *J* = 6.0 Hz, 2H), 7.56 (d, *J* = 8.7 Hz, 2H), 7.36 (t, *J* = 7.6 Hz, 2H), 6.70 (s, 1H), 6.46 (s, 2H), 3.79 (s, 6H). ^{13}C-NMR (100 MHz, DMSO-d_6): δ 160.5, 141.0, 136.6, 136.1, 132.6, 130.8, 129.2, 128.7, 126.9, 124.9, 109.1, 99.0, 55.3. ^{11}B-NMR (128 MHz, DMSO-d_6): δ 30.7. HRMS (ESI): m/z $[M + H]^+$ Calcd for $C_{22}H_{21}B_2O_6$ 403.1526; Found 403.1523.

(10-(3,5-bis(2-(2-(2-methoxyethoxy)ethoxy)ethoxy)phenyl)anthracene-1,8-diyl)diboronic acid 2^{TEG}

In a dry Schlenk, compound **7^{TEG}** (169 mg, 0.261 mmol), bis(neopentyl glycolato)diboron (146 mg, 0.644 mmol), XPhos (10 mg, 0.0208 mmol) and NaOAc (270 mg, 3.3 mmol) were added in 1,4-dioxane (4.5 mL). The resulting suspension was degassed through 3 freeze-pump-thaw cycles and $[Pd_2(dba)_3]$ (14 mg, 0.016 mmol) added to the mixture. The reaction was stirred at 90 °C for 1.5 h. The solvent was removed *in vacuo*. The catalyst was precipitated upon addition of toluene, removed through filtration on celite and the filtrate concentrated. To a solution of the resulting crude mixture in Et_2O (9.6 mL), a solution of diethanolamine (40 µL, 0.409 mmol) in *i*-PrOH (2 mL) was added. The mixture was stirred for 2 h at room temperature. The solution was washed by centrifugation upon addition of Et_2O (4×8 mL) and a solid isolated. The solid was suspended in 1M *aq* HCl (6.4 mL). The mixture

was stirred at room temperature for 2 h. The solid was washed by centrifugation upon addition of H_2O (4×8 mL) and a solid isolated. The solid was dried using a freeze-dryer overnight, yielding compound **2**$^{\mathbf{TEG}}$ (64 mg, 37%) as a white powder. M.p. 113-115°C. FTIR (ATR) ν (cm^{-1}): ν 3344, 2875, 1587, 1429, 1166, 1093, 826. ^{1}H-NMR (400 MHz, DMSO-d_6): δ 9.42 (s, 1H), 8.37 (s, 4H), 7.64 (d, *J* = 6.5 Hz, 2H), 7.57 (d, *J* = 8.8 Hz, 2H), 7.36 (dd, *J* = 8.8, 6.5 Hz, 2H), 6.73 (s, 1H), 6.44 (d, *J* = 2.1 Hz, 2H), 4.13 (t, *J* = 4.2 Hz, 4H), 3.73 (t, *J* = 4.2 Hz, 4H), 3.58-3.56 (m, 4H), 3.52-3.48 (m, 8H), 3.41- 3.38 (m, 4H), 3.20 (s, 6H). ^{13}C-NMR (100 MHz, DMSO-d_6): δ 170.9, 159.7, 141.0, 132.6, 130.8, 128.7, 126.9, 124.9, 109.7, 99.9, 71.3, 70.0, 69.8, 69.6, 69.0, 67.4, 58.12 carbon missing probably due to overlap). ^{11}B-NMR (128 MHz, DMSO-d_6): not detected. HRMS (ESI): m/z $[M + Na]^+$ Calcd for $C_{34}H_{44}B_2NaO_{12}$ 689.2922 Found 689.2921.

(10-((triisopropylsilyl)ethynyl)anthracene-1,8-diyl)diboronic acid 3

To a suspension of compound **12** (90 mg, 0.1545 mmol) in Et_2O (8 mL), a solution of diethanolamine (33 µL, 0.337 mmol) in *i*-PrOH (1.7 mL) was added. The mixture was stirred for 3 h at room temperature. The suspension was filtered and the solid obtained suspended in 1M *aq* HCl (6.4 mL). The mixture was stirred at room temperature for 3 h. The solution was filtered and the solid washed with H_2O (3×5 mL). The solid was dried using a freeze-dryer overnight, yielding desired compound **3** (25 mg, 37%) as a bright yellow powder. M.p. 292-293 °C. FTIR (ATR) ν (cm^{-1}): ν 3326, 2940, 2863, 1366, 1326, 1239, 1115, 1032, 882, 748, 662. ^{1}H-NMR (400 MHz, DMSO-d_6): δ 9.54 (s, 1H), 8.50 (d, *J* = 8.5 Hz, 2H), 8.44 (s, 4H), 7.74 (d, *J* = 6.2 Hz, 2H), 7.64 (t, *J* = 8.5 Hz, 2H), 1.24 (s, 21H). ^{13}C-NMR (100 MHz, DMSO-d_6): δ 132.5, 131.9, 131.6, 131.4, 126.6, 126.4, 115.8, 101.7, 18.7, 10.9 (2 carbon missing probably due to overlap). ^{11}B-NMR (128 MHz, DMSO-d_6): δ 31.3. HRMS (ESI): m/z $[M + H]^+$ Calcd for $C_{25}H_{33}B_2O_4Si$ 447.2338; Found 447.2336.

1,8-dichloro-10-(3,5-dimethoxyphenyl)-10-hydroxyanthracen-9(10H)-one 6

In a dry 2 neck flask, 1-bromo-3,5-dimethoxybenzene **4** (108.5 mg, 0.5 mmol) was dissolved in dry THF (2 mL). 0.5 mL of the resulting solution were added to a second dry two neck flask containing Mg (14 mg, 0.575 mmol) and a crystal of I_2. The suspension was heated up (around 60 °C) until reaching a point in which a transparent suspension was obtained (the iodine disjunction). As soon as no suspension was observed, the rest of the solution containing **4** was added to the solution. The mixture was stirred for 1 h at room temperature. The resulting Grignard suspension was added to a dry two neck flask containing an ice-cold solution of compound **5** (138.5 mg, 0.5 mmol) dissolved in dry THF (3 mL). The reaction was let to reach room temperature stirring overnight. The solvent was removed *in vacuo* and compound **6** was purified by silica gel column chromatography (Cyclohexane/EtOAc 75:25) as a white solid (139 mg, 67%). M.p. 232-233 °C. FTIR (ATR) ν (cm^{-1}): ν 1677, 1587, 1244, 1192, 1151, 1134, 974, 788, 722. ^{1}H-NMR (400 MHz, $CDCl_3$): δ 7.79-7.76 (m, 2H), 7.46-7.44 (m, 4H), 6.35 (d, *J* = 2.2 Hz, 2H), 6.24 (t, *J* = 2.2 Hz, 1H), 3.66 (s, 6H). ^{13}C-NMR (100 MHz, $CDCl_3$): δ 183.4, 161.0, 148.1, 147.4, 133.0, 131.5, 130.5, 124.7, 104.3, 99.2, 74.1, 55.5 (1 peak missing, probably due to overlap).

1,8-dichloro-10-(3,5-dimethoxyphenyl)anthracene 7^{Me}

In a dry 30 mL Schlenk containing a suspension of $LiAlH_4$ (44 mg, 1.152 mmol) in dry Et_2O (4.5 mL) and cooled down at 0 °C was added $BF_3.Et_2O$ (0.329 mL, 2.6 mmol). A solution of **6** (133 mg, 0.48 mmol) in dry CH_2Cl_2 (4.5 mL) was added and the mixture stirred at reflux for 48 h. After cooling using an ice-bath, MeOH (4 mL), H_2O (2 mL) and CH_2Cl_2 (10 mL) were added. The phases were separated, and the aqueous phase extracted with CH_2Cl_2 (2×5 mL). The combined organic layers were washed with brine (10 mL), dried over $MgSO_4$ and filtered. The solvent was removed *in vacuo* and compound $\mathbf{7^{Me}}$ purified by silica gel column

chromatography (Pentane/EtOAc 98:2) as a pale yellow solid (188 mg, 95%). M.p. 224-225°C. FTIR (ATR) ν (cm^{-1}): ν 1592, 1359, 1154, 845, 814, 123, 697. ^{1}H-NMR (400 MHz, $CDCl_3$): δ 9.39 (s, 1H), 7.67 (d, *J* = 8.9 Hz, 2H), 7.63 (d, *J* = 7.3 Hz, 2H), 7.32-7.28 (m, 2H), 6.66-6.65 (m, 1H), 6.56-6.55 (m, 2H), 3.83 (s, 6H). ^{13}C-NMR (100 MHz, $CDCl_3$): δ 160.9, 140.4, 138.5, 132.7, 131.3, 129.2, 126.4, 126.0, 125.6, 121.1, 109.3, 100.1, 55.6. HRMS (ESI): m/z $[M]^+$ Calcd for $C_{22}H_{16}O_2Cl_2$ 382.0527; Found 382.0515.

10-(3,5-bis(2-(2-(2-methoxyethoxy)ethoxy)ethoxy)phenyl)-1,8-dichloro anthracene 7^{TEG}

In a dry Schlenk, compound $\mathbf{7^{Me}}$ (70 mg, 0.182 mmol) was dissolved in dry CH_2Cl_2 (3 mL) and cooled down at -78 °C. BBr_3 (0.5 mL, 0.5 mmol, 1 M in hexane) cooled at -78 °C was added at this temperature. The solution was let to reach room temperature overnight, poured into ice water and extracted with EtOAc (3×5 mL). The organic layers were combined, dried over $MgSO_4$, filtered and evaporated. The residue was precipitated in pentane. In a dry Schlenk, 50 mg of the solid obtained, TEG-OTs (107.5 mg, 0.338 mmol) and K_2CO_3 (77.2 mg, 0.56 mmol) were added to dry DMF (1 mL). The reaction was stirred at 50 °C for 48 h. The mixture was diluted with H_2O (6 mL) and the aqueous suspension extracted with CH_2Cl_2 (3×12 mL). The combined organic layers were dried over $MgSO_4$ and the solvent removed *in vacuo*. Compound $\mathbf{7^{TEG}}$ was purified through silica gel column chromatography (EtOAc/MeOH 99:1) as a brown viscous oil (55 mg, 61%). M.p. 53-54 °C. FTIR (ATR) ν (cm^{-1}): ν 2872, 1592, 1434, 1350, 1169, 1100, 1064, 845, 815. ^{1}H-NMR (400 MHz, $CDCl_3$): δ 9.36 (s, 1H), 7.64-7.60 (m, 4H), 7.28-7.26 (m, 2H), 6.67 (s, 1H), 6.54 (d, *J* = 2.0 Hz, 2H), 4.13 (t, *J* = 4.7 Hz, 4H), 3.85 (t, *J* = 4.7 Hz, 4H), 3.74-3.71 (m, 4H), 3.68-3.65 (m, 4H), 3.64-3.60 (m, 4H), 3.53-3.50 (m, 4H), 3.34 (s, 6H). ^{13}C-NMR (100 MHz, $CDCl_3$): δ 160.0, 140.2, 138.5, 132.6, 131.2, 129.2, 126.5, 126.0, 125.6, 121.1, 110.2, 101.3, 72.0, 71.0, 70.8, 70.7,

69.8, 67.8, 59.2. HRMS (MALDI-TOF): m/z $[M]^+$ Calcd for $C_{34}H_{40}O_8Cl_2$ 646.2100; Found 646.2095.

2,2'-(10-(3,5-dimethoxyphenyl)anthracene-1,8-diyl)bis(5,5-dimethyl-1,3,2-dioxaborinane) 8^{Me}

In a dry Schlenk, compound **7^{Me}** (100 mg, 0.261 mmol), bis(neopentyl glycolato)diboron (146 mg, 0.644 mmol), XPhos (10 mg, 0.0208 mmol) and NaOAc (270 mg, 3.3 mmol) were added in 1,4-dioxane (4.5 mL). The resulting suspension was degassed through 3 freeze-pump-thaw cycles and $[Pd_2(dba)_3]$ (14 mg, 0.016 mmol) added to the mixture. The reaction was stirred at 90 °C for 1 h. The solvent was removed *in vacuo.* The catalyst was precipitated by addition of toluene and removed through filtration on celite. The filtrate was concentrated and precipitation in Et_2O yielded compound **8^{Me}** as a light-yellow powder (80 mg, 57%). M.p. 292-293 °C. FTIR (ATR) ν (cm^{-1}): ν 1584, 1283, 1248, 1138, 752, 675. ^{1}H-NMR (400 MHz, $CDCl_3$): δ 10.26 (s, 1H), 8.03 (d, *J* = 6.0 Hz, 2H), 7.76 (d, *J* = 8.7 Hz, 2H), 7.31 (dd, *J* = 8.7, 6.6 Hz, 2H), 6.64-6.60 (m, 1H), 6.56-6.55 (m, 2H), 3.98 (s, 8H), 3.81 (s, 6H), 1.17 (s, 12H). ^{13}C-NMR (100 MHz, $CDCl_3$): δ 160.7, 142.1, 137.3, 134.3, 134.1, 129.8, 129.5, 128.3, 124.5, 109.6, 99.7, 90.2, 72.8, 55.6, 32.1, 22.3. ^{11}B-NMR (128 MHz, $CDCl_3$): 27.0.

4,5-dichloroanthracen-9-yl trifluoromethanesulfonate 9

In a dry 50 mL flask containing a suspension of compound **10** (200 mg, 0.763 mmol) in CH_2Cl_2 (4.2 mL), DBU (228.6 µl, 1.527 mmol) was added dropwise over a period of 90 min (26 µL every 10 min). Trifluoromethanesulfonic anhydride (0.954 mmol, 160.5 µL, 1M in CH_2Cl_2) was slowly added over a period of 90 min (110 µL every 10 min). The reaction was stirred at 0 °C for 10 min, after which additional trifluoromethanesulfonic anhydride (200 µL) was added and the reaction stirred for 45 min. H_2O (3 mL) was added to the reaction vessel and the resulting mixture stirred overnight. The phases were separated, and the aqueous layer

extracted with CH_2Cl_2 (3×20 mL). The organic layers were combined, dried over $MgSO_4$, filtered and evaporated. The resulting crude was purified through silica gel column chromatography (CH_2Cl_2/Cyclohexane 1:1) to yield compound **9** as a crystalline yellow solid (227 mg, 75%). M.p. 123-125 °C. FTIR (ATR) ν (cm^{-1}): ν 1398, 1323, 1207, 1126, 891, 801, 726, 727. ^{1}H-NMR (400 MHz, $CDCl_3$): δ 9.39 (s, 1H), 8.16 (d, *J* = 8.9 Hz, 2H), 7.71 (d, *J* = 7.3 Hz, 2H), 7.58 (dd, *J* = 8.9, 7.3 Hz, 2H). ^{13}C-NMR (100 MHz, $CDCl_3$): δ 140.2, 133.1, 129.6, 128.1, 126.9, 125.9, 122.6, 120.5 (carbon bearing the fluorine atoms missing). HRMS (ESI): m/z $[M + H]^+$ Calcd for $C_{15}H_8O_3SF_3Cl_2$ 394.9517; Found 394.9512.

4,5-dichloroanthracen-9(10H)-one 10

In a 500 mL 2 neck flask, compound **5** (2.77 g, 9.99 mmol) was suspended in DMF (100 mL) and H_2O (100 mL). The resulting mixture was heated at 30 °C and $Na_2S_2O_4$ (1.739 g, 99.9 mmol) was added under argon. Every 15 min the temperature was raised by 10 °C, reaching 90 °C in 1.5 h. The reaction was stirred at 90 °C for 3 h. The mixture was cooled down at room temperature and CH_2Cl_2 (100 mL) was added. The phases were separated and the aqueous layer extracted with CH_2Cl_2 (1×200 mL; 2×150 mL). The organic layers were collected, dried over $MgSO_4$, filtered and evaporated. The crude material was purified through silica gel column chromatography (CH_2Cl_2/Cyclohexane 1:1), to yield compound **10** as a white crystalline solid (2.533 g, 96%). M.p. 187-189 °C. FTIR (ATR) ν (cm^{-1}): ν 1656, 1589, 1308, 1283, 1133, 818, 740. ^{1}H-NMR (400 MHz, $CDCl_3$): δ 8.29 (dd, *J* =7.8, 1.1 Hz, 2H), 7.71 (dd, *J* =7.8,1.1 Hz, 2H), 7.46 (t, *J* = 7.8, 2H), 4.25 (s, 2H). ^{13}C-NMR (100 MHz, $CDCl_3$): δ 182.9, 137.5, 134.3, 133.9, 133.0, 128.2, 126.5, 29.6. HRMS (ESI): m/z $[M + H]^+$ Calcd for $C_{14}H_9OCl_2$ 263.0024; Found 263.0026. Spectral characterization agrees with previously reported data.[46,47]

((4,5-dichloroanthracen-9-yl)ethynyl)diisopropyl(methyl)silane 11

In a dry Schlenk containing a suspension of compound **9** (980 mg, 2.49 mmol) and NaOAc (2.577 g, 31.41 mmol) in THF (70 mL), CuI (47.5 mg, 0.249 mmol) and PPh_3 (261.24 mg, 0.996 mmol) were added. 3 freeze-pump-thaw cycles were performed and [$Pd(PPh_3)_4$] (288 mg, 0.249 mmol) added at room temperature. After an additional freeze-pump-thaw cycle triisopropylacetylene (614.5 μL, 2.739 mmol) was added and the reaction stirred at 60 °C overnight. The solvent was removed *in vacuo*. The crude material was purified through silica gel column chromatography (Cyclohexane) to yield **11** as a crystalline yellow solid (936 mg, 88%). M.p. 169-171°C. FTIR (ATR) ν (cm^{-1}): ν 2941, 2864, 1441, 1339, 1146, 994, 880, 736, 677. ^{1}H-NMR (400 MHz, $CDCl_3$): δ 9.26 (s, 1H), 8.55 (d, *J* = 8.5 Hz, 2H), 7.64 (d, *J* = 7.1 Hz, 2H), 7.50 (dd, *J* = 8.5, 7.1 Hz, 2H), 1.26 (s, 21H). ^{13}C-NMR (100 MHz, $CDCl_3$): δ 134.1, 133.1, 129., 126.9, 126.4, 126.2, 121.9, 119.5, 104.6, 102.7, 19.0, 11.6. HRMS (ESI): m/z [M + H]$^+$ Calcd for $C_{25}H_{29}SiCl_2$ 427.1410; Found 427.1406.

((4,5-bis(5,5-dimethyl-1,3,2-dioxaborinan-2-yl)anthracen-9-yl)ethynyl) triisopropylsilane 12

In a dry Schlenk, compound **11** (556 mg, 1.300 mmol), bis(neopentyl glycolato)diboron (725 mg, 3.211 mmol), XPhos (50 mg, 0.104 mmol) and NaOAc (1.345 g, 16.400 mmol) were added in dry 1,4-dioxane (4.5 mL). The resulting suspension was degassed through 3 freeze-pump-thaw cycles and [$Pd_2(dba)_3$] (14 mg, 0.016 mmol) added to the mixture. The reaction was stirred at 90 °C for 1 h. The solvent was removed *in vacuo.* The catalyst was precipitated upon addition of toluene and removed through filtration on celite. The filtrate was concentrated *in vacuo.* A white powder was precipitated upon addition of *n*-hexane and removed through filtration on celite. The solvent was removed *in vacuo,* yielding the desired compound **12** (151 mg, 20%) as a pale-yellow powder. M.p. 97-100 °C. FTIR (ATR) ν (cm^{-1}): ν 2957, 2933, 1417, 1385, 1341, 1289, 1249, 1142, 663. ^{1}H-NMR (400 MHz, $CDCl_3$): δ 10.25

(s, 1H), 8.73 (d, *J* = 8.5 Hz, 2H), 8.08 (d, *J* = 6.6 Hz, 2H), 7.54 (t, *J* = 8.5 Hz, 2H), 3.97 (s, 8H), 1.27-1.26 (m, 21H), 1.16 (s, 12H). ^{13}C-NMR (100 MHz, $CDCl_3$): δ 134.8, 134.1, 132.7, 131.8, 129.7, 125.9, 104.4, 88.9, 72.8, 32.1, 22.3, 19.1, 11.7 (2 peaks missing probably due to overlap). ^{11}B-NMR (128 MHz, $CDCl_3$): δ 27.63.

4,5-dichloro-10-hydroxyanthracen-9(10H)-one 13

In a 500 mL flask containing a suspension of compound **5** (2.77 g, 9.99 mmol) in DMF (100 mL) and H_2O (100 mL), $Na_2S_2O_4$ (1.739 g, 99.9 mmol) was added under argon. The reaction was stirred at room temperature overnight. The solvent was removed *in vacuo*. The crude was dissolved in CH_2Cl_2 (200 mL) and H_2O (100 mL) added. The phases were separated and the aqueous layer was extracted with CH_2Cl_2 (3×150 mL). The organic layers were combined, dried over $MgSO_4$, filtered and evaporated. The crude material was purified through silica gel column chromatography (CH_2Cl_2/Cyclohexane 1:1), to yield compound **13** as an orange powder (2.56 g, 98%). M.p. 202-205 °C. FTIR (ATR) ν (cm^{-1}): ν 3513, 1657, 1574, 1309, 1132, 1000, 791, 753, 721. ^{1}H-NMR (400 MHz, $CDCl_3$): δ 8.20 (dd, *J* = 8.0, 1.1 Hz, 2H), 7.73 (dd, *J* = 7.8, 1.1 Hz, 2H), 7.50 (dd, *J* = 8.0, 7.8 Hz, 2H), 6.39 (s, 1H) (OH signal missing). ^{13}C-NMR (100 MHz, $CDCl_3$): δ 182.7, 138.4, 135.1, 135.0, 132.8, 130.2, 126.7, 61.8. HRMS (ESI): m/z $[M + H]^+$ Calcd for $C_{14}H_9O_2Cl_2$ 278.9974; Found: 278.9970.

(9r,10r)-1,8-dichloro-9,10-dihydroanthracene-9,10-diol 14

In a two necked flask under argon, a solution of compound **5** (400 mg, 1.433 mmol) in dry MeOH (7.2 mL) was cooled to 0 °C and $NaBH_4$ (217 mg, 5.732 mmol) was added in small portions in order to prevent the temperature to rise. The resulting mixture was stirred between 0-5 °C for 1 h. The crude was poured into ice water and desired compound **14** precipitated as a white powder, filtered off and washed with H_2O (363 mg, 90%). M.p. 157-160 °C. FTIR (ATR) ν (cm^{-1}): ν 3403, 1449, 1192, 959, 869, 786, 692. ^{1}H-NMR (400 MHz, CD_3OD): δ

7.74 (dd, *J* = 7.2, 1.0 Hz, 2H), 7.39-7.36 (m, 4H), 6.66 (s, 1H), 5.87 (s, 1H) (OH signal missing). ^{13}C-NMR (100 MHz, CD_3OD): δ 146.4, 134.8, 134.6, 130.2, 129.1, 124.5, 67.9, 64.4. HRMS (ESI): m/z $[M + Na]^+$ Calcd for $C_{14}H_{10}Cl_2NaO_2$ 302.9950; Found 302.9945.

(9s,10s)-1,8-dichloro-9,10-dihydroanthracene-9,10-diol 15

To a solution of 1,8-dichloroanthracene-9,10-dione **5** (277 mg, 1 mmol) in dry THF (30 mL) was added dropwise DIBAH (3 mL, 3 mmol, 1 M in hexane). The reaction mixture was stirred for 5 h, followed by the addition of saturated aqueous Rochelle's salt solution (25 mL). The resulting mixture was stirred at room temperature overnight. The mixture was extracted with EtOAc (3×25 mL), the organic layers were combined, dried over $MgSO_4$, filtered and evaporated. Compound **15** was purified through silica gel column chromatography (Cyclohexane/EtOAc 8:2) and isolated as a white powder (252 mg, 89%). M.p. 207-210 °C. FTIR (ATR) ν (cm^{-1}): ν 3346, 1661, 1581, 1451, 1176, 955, 810, 763. ^{1}H-NMR (400 MHz, CD_3OD): δ 7.49-7.44 (m, 4H), 7.36 (t, *J* = 7.8 Hz, 2H), 6.37 (s, 1H), 5.51 (s, 1H) (OH signals missing). ^{13}C-NMR (100 MHz, CD_3OD): δ 142.7, 137.3, 135.4, 130.8, 130.6, 129.2, 71.3, 64.3. HRMS (ESI): m/z $[M]^+$ Calcd for $C_{14}H_{10}Cl_2NaO_2$ 302.9950; 302.9950.

Acknowledgments

D.B. gratefully acknowledge the EU through the SGt-ERC (project: COLORLANDS), MSCA-RISE (project: INFUSION), MSCA-ITN (project PHOTOTRAIN), IA-H2020 (project: DecoChrom) funding schemes for the financial support. A.S. thanks the DecoChrom project for his post-doctoral fellowship.

Supporting Information

Synthetic pathways and protocol for compound **1**, DFT explanations, ^{1}H, ^{13}C and ^{11}B NMR spectra, and crystallographic data. This material is available free of charge via the Internet.

References

1. Hall, D. G. *Boronic Acids: Preparation and Applications in Organic Synthesis and Medicine*: Weinheim, Germany, 2005.
2. Suzuki, A. *Angew. Chem., Int. Ed.* 2011; *50*: 6722.
3. Mora, M.; Jimenez-Sanchidrian, C.; Ruiz, J. R. *Curr. Org. Chem.* 2012; *16*: 1128.
4. Lennox, A. J. J.; Lloyd-Jones, G. C. *Chem. Soc. Rev.* 2014; *43*: 412.
5. Heravi, M. M.; Malmir, M.; Moradi, R. *Curr. Org. Chem.* 2019; *23*: 2469.
6. Nishiyabu, R.; Kubo, Y.; James, T. D.; Fossey, J. S. *Chem. Commun.* 2011; *47*: 1106.
7. Sun, X.; James, T. D. *Chem. Rev.* 2015; *115*: 8001.
8. Brooks, W. L. A.; Sumerlin, B. S. *Chem. Rev.* 2016; *116*: 1375.
9. Akgun, B.; Hall, D. G. *Angew. Chem., Int. Ed.* 2018; *57*: 13028.
10. Rowan, S. J.; Cantrill, S. J.; Cousins, G. R. L.; Sanders, J. K. M.; Stoddart, J. F. *Angew. Chem., Int. Ed.* 2002; *41*: 898.
11. Lehn, J.-M. *Chem. Soc. Rev.* 2007; *36*: 151.
12. Jin, Y.; Yu, C.; Denman, R. J.; Zhang, W. *Chem. Soc. Rev.* 2013; *42*: 6634.
13. Wilson, A.; Gasparini, G.; Matile, S. *Chem. Soc. Rev.* 2014; *43*: 1948.
14. Fournier, J.-H.; Maris, T.; Wuest, J. D.; Guo, W.; Galoppini, E. *J. Am. Chem. Soc.* 2003; *125*: 1002.
15. Maly, K. E.; Malek, N.; Fournier, J.-H.; Rodriguez-Cuamatzi, P.; Maris, T.; Wuest, J. D. *Pure Appl. Chem.* 2006; *78*: 1305.
16. Adamczyk-Wozniak, A.; Cyranski, M. K.; Dabrowska, A.; Gierczyk, B.; Klimentowska, P.; Schroeder, G.; Zubrowska, A.; Sporzynski, A. *J. Mol. Struct.* 2009; *920*: 430.

17. Regueiro-Figueroa, M.; Djanashvili, K.; Esteban-Gomez, D.; de Blas, A.; Platas-Iglesias, C.; Rodriguez-Blas, T. *Eur. J. Org. Chem.* 2010: 3237.

18. Cyranski, M. K.; Klimentowska, P.; Rydzewska, A.; Serwatowski, J.; Sporzynski, A.; Stepien, D. K. *CrystEngComm* 2012; *14*: 6282.

19. Adamczyk-Wozniak, A.; Brzozka, Z.; Dabrowski, M.; Madura, I. D.; Scheidsbach, R.; Tomecka, E.; Zukowski, K.; Sporzynski, A. *J. Mol. Struct.* 2013; *1035*: 190.

20. Campos-Gaxiola, J. J.; Vega-Paz, A.; Roman-Bravo, P.; Hopfl, H.; Sanchez-Vazquez, M. *Cryst. Growth Des.* 2010; *10*: 3182.

21. Rettig, S. J.; Trotter, J. *Can. J. Chem.* 1977; *55*: 3071.

22. Cyranski, M. K.; Jezierska, A.; Klimentowska, P.; Panek, J. J.; Sporzynski, A. *J. Phys. Org. Chem.* 2008; *21*: 472.

23. Durka, K.; Jarzembska, K. N.; Kamiński, R.; Luliński, S.; Serwatowski, J.; Woźniak, K. *Cryst. Growth Des.* 2013; *13*: 4181.

24. Adamczyk-Wozniak, A.; Cyranski, M. K.; Durka, K.; Gozdalik, J. T.; Klimentowska, P.; Rusiecki, R.; Sporzynski, A.; Zarzeczanska, D. *Crystals* 2019; *9*: 109.

25. Rodríguez-Cuamatzi, P.; Vargas-Díaz, G.; Höpfl, H. *Angew. Chem., Int. Ed.* 2004; *43*: 3041.

26. Pedireddi, V. R.; SeethaLekshmi, N. *Tetrahedron Lett.* 2004; *45*: 1903.

27. SeethaLekshmi, S.; Varughese, S.; Giri, L.; Pedireddi, V. R. *Cryst. Growth Des.* 2014; *14*: 4143.

28. TalwelkarShimpi, M.; Oeberg, S.; Giri, L.; Pedireddi, V. R. *Cryst. Growth Des.* 2017; *17*: 6247.

29. Rodriguez-Cuamatzi, P.; Luna-Garcia, R.; Torres-Huerta, A.; Bernal-Uruchurtu, M. I.; Barba, V.; Hopfl, H. *Cryst. Growth Des.* 2009; *9*: 1575.

30. Campillo-Alvarado, G.; Brannan, A. D.; Swenson, D. C.; MacGillivray, L. R. *Org. Lett.* 2018; *20*: 5490.

31. Georgiou, I.; Kervyn, S.; Rossignon, A.; De Leo, F.; Wouters, J.; Bruylants, G.; Bonifazi, D. *J. Am. Chem. Soc.* 2017; *139*: 2710.

32. Djurdjevic, S.; Leigh, D. A.; McNab, H.; Parsons, S.; Teobaldi, G.; Zerbetto, F. *J. Am. Chem. Soc.* 2007; *129*: 476.

33. Leigh, D. A.; Robertson, C. C.; Slawin, A. M. Z.; Thomson, P. I. T. *J. Am. Chem. Soc.* 2013; *135*: 9939.

34. Blight, B. A.; Hunter, C. A.; Leigh, D. A.; McNab, H.; Thomson, P. I. T. *Nat. Chem.* 2011; *3*: 244.

35. Sijbesma, R. P.; Meijer, E. W. *Chem. Commun.* 2003: 5.

36. Wilson, A. J. *Soft Matter* 2007; *3*: 409.

37. Beijer, F. H.; Kooijman, H.; Spek, A. L.; Sijbesma, R. P.; Meijer, E. W. *Angew. Chem., Int. Ed.* 1998; *37*: 75.

38. Zimmerman, S. C.; Corbin, P. S. *Struct. Bonding* 2000; *96*: 63.

39. Sijbesma, R. P.; Beijer, F. H.; Brunsveld, L.; Folmer, B. J. B.; Hirschberg, J. H. K. K.; Lange, R. F. M.; Lowe, J. K. L.; Meijer, E. W. *Science* 1997; *278*: 1601.

40. Marangoni, T.; Bonifazi, D. *Nanoscale* 2013; *5*: 8837.

41. Wada, T.; Muckerman, J. T.; Fujita, E.; Tanaka, K. *Dalton Trans.* 2011; *40*: 2225.

42. De Vries, J. G.; Kellogg, R. M. *J. Org. Chem.* 1980; *45*: 4126.

43. Gassman, P. G.; Rasmy, O. M.; Murdock, T. O.; Saito, K. *J. Org. Chem.* 1981; *46*: 5455.

44. Prinz, H.; Wiegrebe, W.; Mueller, K. *J. Org. Chem.* 1996; *61*: 2853.

45. Cristol, S. J. *Acc. Chem. Res.* 1971; *4*: 393.

46. Karama, U.; Sultan, M. A.; Ghabour, H. A.; Fun, H. K.; Kh. Warad, I. *Z. Kristallogr. - New Cryst. Struct.* 2013; *228*: 405.

47. Tauchert, M. E.; Kaiser, T. R.; Goethlich, A. P. V.; Rominger, F.; Warth, D. C. M.; Hofmann, P. *ChemCatChem* 2010; *2*: 674.

Graphical abstract:

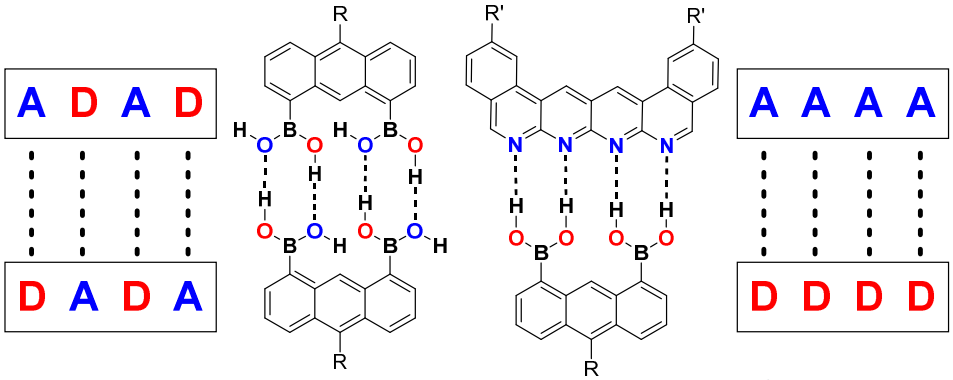

1,8,10-Trisubstituted anthracenyl hydrocarbons: towards versatile scaffolds for multiple-H-bonded recognition arrays.

Silvia Forensi,[1] Antoine Stopin,[2,3] Federica de Leo,[1] Johan Wouters,[1] Davide Bonifazi[2,3]*

Dr. S. Forensi, Dr. F. de Leo, Prof. J. Wouters
Department of Chemistry, University of Namur, Rue de Bruxelles 61, 5000 Namur, Belgium

Dr. A. Stopin, Prof. Dr. D. Bonifazi
School of Chemistry, Cardiff University, Main Building, Park Place, CF10 3AT, Cardiff, United Kingdom; E-mail: BonifaziD@cardiff.ac.uk

Dr. A. Stopin, Prof. Dr. D. Bonifazi
Institute of Organic Chemistry, Faculty of Chemistry, University of Vienna, Währinger Str. 38, 1090, Vienna, Austria; E-mail: davide.bonifazi@univie.ac.at

Dedicated to Professor Nuno Maulide on the occasion of his receipt of the Tetrahedron Young Investigator Award.

Keywords: anthracene, polycyclic aromatic hydrocarbons, boronic acids, hydrogen-bonds

Abstract: In this work, we describe the synthesis of 1,8,10-trisubstituted anthracenyl scaffolds that, bearing boronic acid functionalities, can act as multiple H-bonding donor systems. The trisubstituted anthracenyl derivatives are synthesized following two main synthetic pathways. Whereas in the first approach trisubstituted anthracenyl derivatives are prepared through the regioselective addition of the relevant organomagnesium nucleophile to 1,8-dichloroanthraquinone, in the second avenue a triflate-bearing anthracene is prepared by reduction of the anthraquinone into the anthrone precursor and functionalized through metal-catalysed cross-coupling reactions. Complementary studies of the $Na_2S_2O_4$-mediated reduction of 1,8-dichloroanthraquinone allowed to shed further light on the possible mechanism of formation of the anthrone precursor, suggesting the presence of a *cis*-diol

intermediate undergoing antiperiplanar elimination. Solid-state X-ray diffraction investigations of the bisboronic acids show that the molecules self-assemble into dimers through the formation of four H-bonds established between the *anti-syn* conformers of the boronic acid moieties. ^{1}H-NMR titrations between bisboronic acids and tetra H-bond acceptor, diisoquinolino-naphthyridine, showed a significant shift of the -B(O*H*)$_2$ proton resonances, suggesting the presence of H-bonding interactions between both molecules.

1. Introduction

Organoboronic acids are one of the most important functional groups used in organic chemistry.[1] They are commonly used as organometallic species in Pd-catalysed Suzuki cross-coupling reactions,[2-5] in sensing,[6-9] and in dynamic covalent chemistry to form boronate esters.[10-13] In the recent years, organoboronic acids have also been proposed as versatile H-bonding donors.[14-19] Depending on the type of conformation adopted by the boronic acid functionality, i.e. *syn-syn*, *syn-anti* and *anti-anti*, they can form different non-covalent H-bonded arrays both in solution and in the solid state.[20] For instance, in the solid state phenylboronic acid undergoes formation of doubly-H-bonded dimers (DA-AD-type), in which the boronic acid moieties adopt a *syn-anti* conformation. The dimers are organised in tapes through the formation of lateral intermolecular H-bonds.[21,22] The same type of DA-AD interactions led to the formation of H-bonded polymers between phenylenediboronic acid whether the two moieties are located in the ortho,[23] meta[24] or para positions.[25] *Pedireddi et al.* also reported the formation of supramolecular assemblies of arylboronic acids with 4,4'-bipyridine.[26-28] Similarly, *Höpfl* and co-workers reported H-bonded polymers between 4,4'-bipyridine and different types of boronic acids.[29] More recently, *MacGillivray* and co-workers exploited the *syn-syn* conformer of boronic acid functionalities to organize 1,2-bis(4-pyridyl)ethylene in the solid state, and trigger a [2+2] photodimerization to yield *rctt*-tetrakis(4-pyridyl)cyclobutane stereoselectively (Figure 1).[30] Our group also reported the use of boronic acids to form doubly H-bonded complexes (DD-AA).[31] Cocrystallization of various arylboronic acids with either 1,8-naphtyridine or 5,6,11,12-tetraazanaphthacene yielded discrete H-bonded complexes, in which the boronic acid moiety are engaged in frontal H-bonding interactions through the *syn-syn* conformer (Figure 1). Notably, H-bonded polymers could be obtained with 1,4-diphenylboronic acid with 5,6,11,12-

tetraazanaphthacene.[31] However, to the best of our knowledge no examples of multiple H-bonded arrays involving boronic acids have been reported so far both in solution and in the solid state.

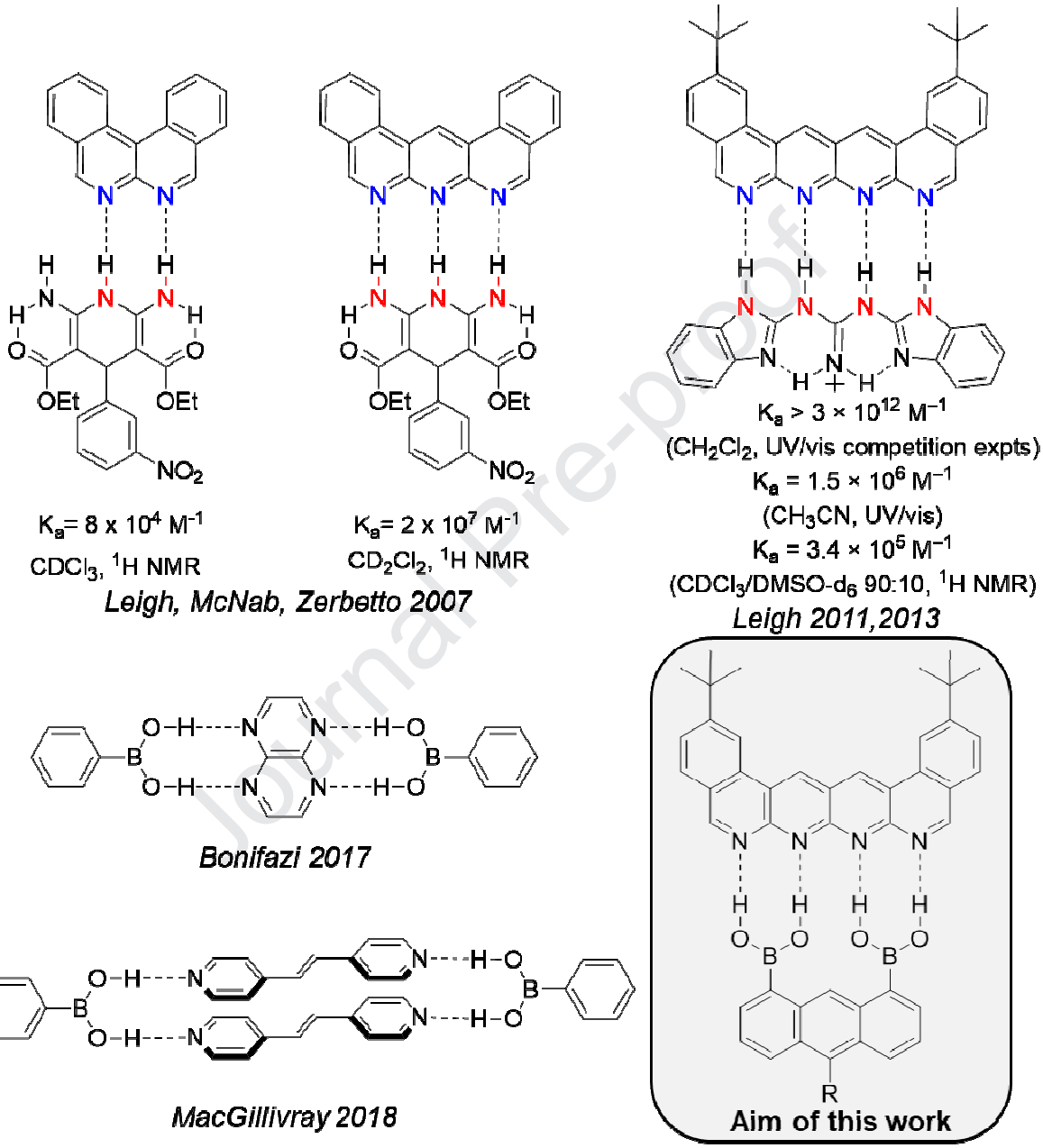

Figure 1. Common multiple H-bonded complexes[32-34,30,31] with (below) and without (above) boronic acids.

Due to their high directionality, selectivity, and reversibility, multiple *H*-bonding arrays are one of the most exploited non-covalent interactions for the preparation of self-assembled

functional organic architectures. In particular, linear *H*-bonded arrays have been extensively used to self-assemble and self-organise functional molecules into well-defined supramolecular architectures.[35-40] Through the demonstration with key examples in the field,[32,34,33] it has been shown that increasing the number of H-bonds in D-type arrays, the strength of association of is dramatically enhanced (Figure 1).[32,34,33] It is with this idea in mind that in this paper we describe our efforts to prepare suitable molecular structures that, bearing two boronic acid functionalities, could act as versatile scaffolds for preparing multiple H-bonded complexes. In particular, we have envisioned the preparation of *peri*-substituted anthracenyl derivatives that, bearing two frontal boronic acids at positions 1 and 8, could undergo formation of quadruple H-bonding interactions in the presence of a suitable acceptor (Figure 1).

2. Results and discussion

2.1 Design of the H-bonding systems: theoretical calculations

We began our investigation with the design of the boronic acid derivatives as H-bonding donors. Capitalizing on the DFT calculation, we modelled a substituted anthracenyl structure bearing boronic acids at *peri*-positions 1 and 8. Geometry optimization of the anthracenyl scaffolds was performed using DFT calculations at the B3LYP/6-311G** level of theory. In the optimized structure both boronic acid functionalities adopt a *syn-syn* conformation, arranging the acidic protons in a DDDD-type array. Notably, the non-acidic anthracenyl CH moiety in position 9 likely hampers the acid functionalities to be fully co-planar with the aromatic core (Figure 2a). When contacted to diisoquinolino-naphthyridine H-bond acceptor (AAAA), single point energy calculation showed that a highly stabilized quadrupole H-bonded complex (DDDD-AAAA) is formed with a predicted ΔH of -32.63 kcal/mol (Figure 2b). It is noteworthy to indicate that this value is superior to that reported for the formation of

doubly H-bonded dimers of phenylboronic acid with naphthyridine of -20.41 kcal/mol.[31] Encouraged by these predictive theoretical results, we planned the synthesis of the anthracenyl derivatives shown in Figure 2c. As we have anticipated limited solubility of bis-boronic acids in common organic solvents, anthracenyl cores bearing different substituents at position 10 have been prepared. The synthesis of H-bonding acceptor compound **1** (AAAA) was accomplished following a protocol reported in the literature (see also SI).[34]

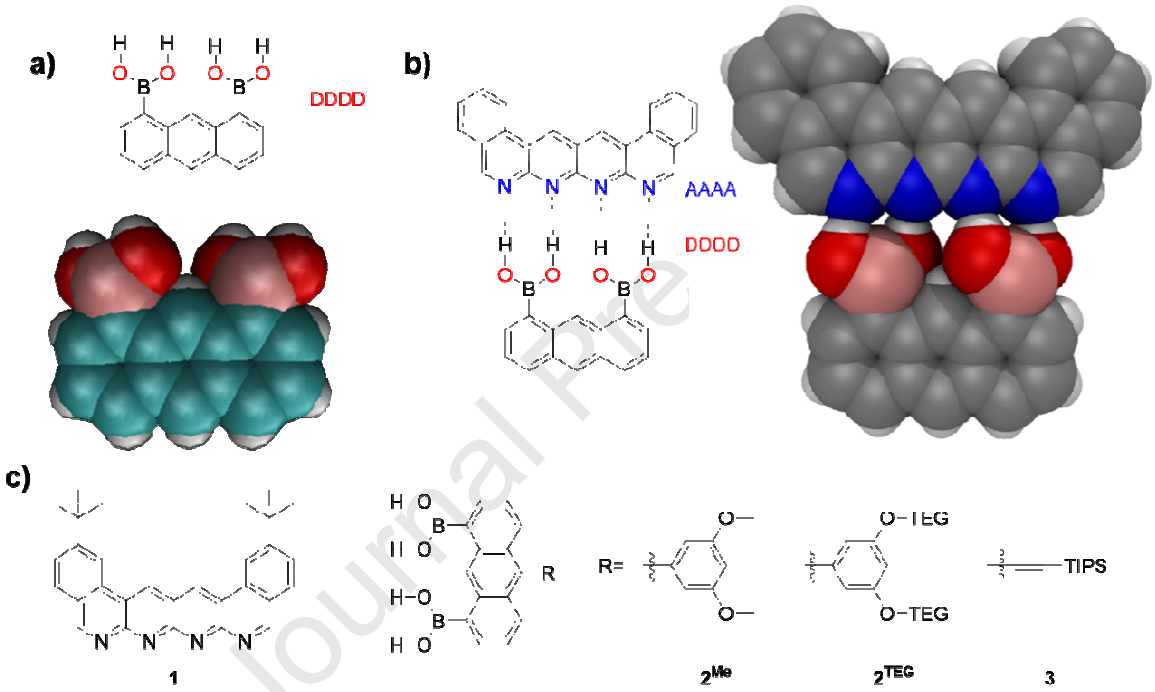

Figure 2. a) B3LYP optimized geometry of the donor backbone, **b)** B3LYP optimized geometry of the 4 H-bonded complex and **c)** structure of the target molecules.

2.2 Synthesis of three-substituted peri-functionalized anthracenyl scaffolds bearing H-bonding boronic acids.

Our investigations began with the synthesis of the H-bonding donor anthracenyl derivatives **2**^{Me}, **2**^{TEG}, and **3** each featuring a different solubilising group at position 10. Starting with compound **2**^{Me} (Scheme 1), bromo-derivative **4** was first reacted with Mg in THF to form its Grignard derivative that reacting with anthraquinone **5** at position 10, yielded hydroxyl-

bearing intermediate **6** in 67% yield. The structure of the addition product could be unambiguously determined by X-ray diffraction of single crystals obtained through evaporation of a solution of **6** in $CHCl_3$ (Figure 3a). As shown by the X-ray structure, molecule **6** adopts a puckered conformation, with the hydroxyl group H-bonded to a carbonyl group ($O_1\square\square\square O_2$ = 2.812(3) Å) of a neighbouring molecule in the crystal lattice. Halogen-halogen ($Cl_1\square\square\square Cl_2$ = 3.424(15) Å) and halogen-oxygen ($Cl_1\square\square\square O_2$ = 3.305(3) Å) short contacts were also observed. Reduction of ketone **6** with $LiAlH_4$ followed by addition of $BF_3{\cdot}Et_2O$ gave trisubstituted anthracenyl derivative $\mathbf{7^{Me}}$ in 95 % yield.

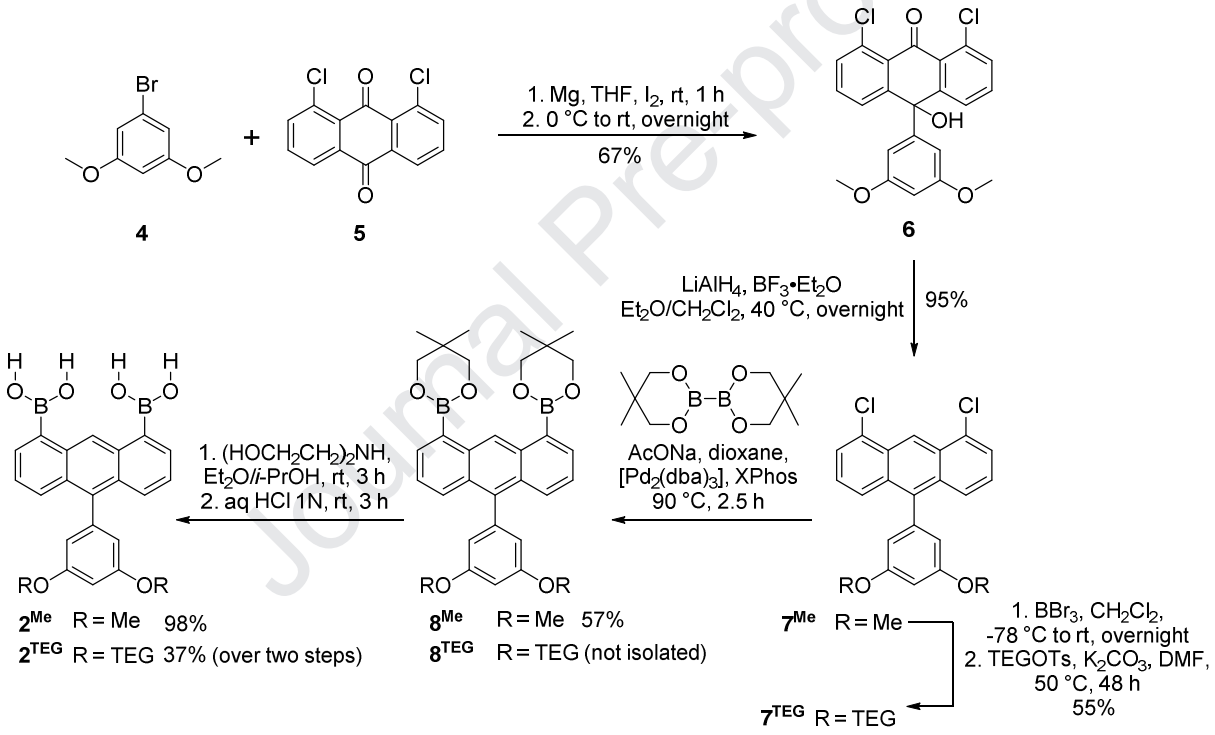

Scheme 1. Synthetic pathway to target anthracenyl derivatives $\mathbf{2^R}$.

Building on a literature protocol developed by *Tanaka*, *Wada* and co-workers, [41] *Miyaura* borylation of anthracene $\mathbf{7^{Me}}$ using bis(neopentylglycolato)diboron in the presence of NaOAc, $[Pd_2(dba)_3]$ and XPhos in 1,4-dioxane at 90 °C led to the formation of di-boronate ester $\mathbf{8^{Me}}$ in 57% yield. Transesterification with diethanolamine, followed by hydrolysis with HCl, led to diboronic acid $\mathbf{2^{Me}}$ in 94% yield. Notably, molecule $\mathbf{2^{Me}}$ proved to be soluble only in DMSO.

In addition to classical ^{1}H- and ^{13}C-NMR characterizations, the structures of the boronic acid derivative was confirmed by X-ray diffraction analysis of single crystals (for molecule **2^{Me}** see section 2.5). Suitable transparent crystals of diboronate **8^{Me}** for X-ray diffraction analysis were obtained from slow evaporation of a solution of $CHCl_3$ (Figure 3b). Pleasingly, the X-ray structure of compound **8^{Me}** shows that the two boronate ester moieties are fundamentally coplanar (dihedral angles O_1-B_1-C_1-C_6 = 17.6(5)° and O_2-B_1-C_1-C_2 = 16.7(5)°) with the anthracenyl scaffold. On the other hand, the aryl substituent is perpendicular to the polycyclic aromatic core (dihedral angle C_5-C_8-C_9-C_{10} = 88.5(4)°).

Figure 3. a) X-ray crystal structure of compound **6**; space group: P-2_1/n. **b)** X-ray crystal structure of compound **8^{Me}**; space group: Pnma. H atoms are omitted except for OH. Atom colours: green Cl, pink B, red O, grey C, white H

To improve the solubility of diboronic acid **2^{Me}** in organic solvents, molecular analogue **2^{TEG}** bearing two triethylene glycol tails was also prepared (Scheme 1**Error! Reference source not found.**). In this case, demethylation of intermediate **7^{Me}** in the presence of BBr_3 in

CH_2Cl_2 followed by alkylation with TEG-OTs under basic conditions led to compound $\mathbf{7}^{\mathbf{TEG}}$ in 55% yield. Following the protocols (*i.e., Miyaura* borylation and transesterification reactions followed by hydrolysis) described previously for installing the boronic acid moieties in molecule $\mathbf{2}^{\mathbf{Me}}$, we prepared target molecule $\mathbf{2}^{\mathbf{TEG}}$ in 37% yield over the two steps. Although the preparative route described so far led to the formation of the desired target molecules, this synthetic strategy is limited by the preparation of a suitable organometallic nucleophile. A more versatile synthetic approach would be one that allows the insertion of any substituents at position 10 through a metal-catalysed cross-coupling reaction. Indulging this line of thought, we turned our attention on anthracene derivative **9** (Scheme 2) as the key intermediate for the new route.

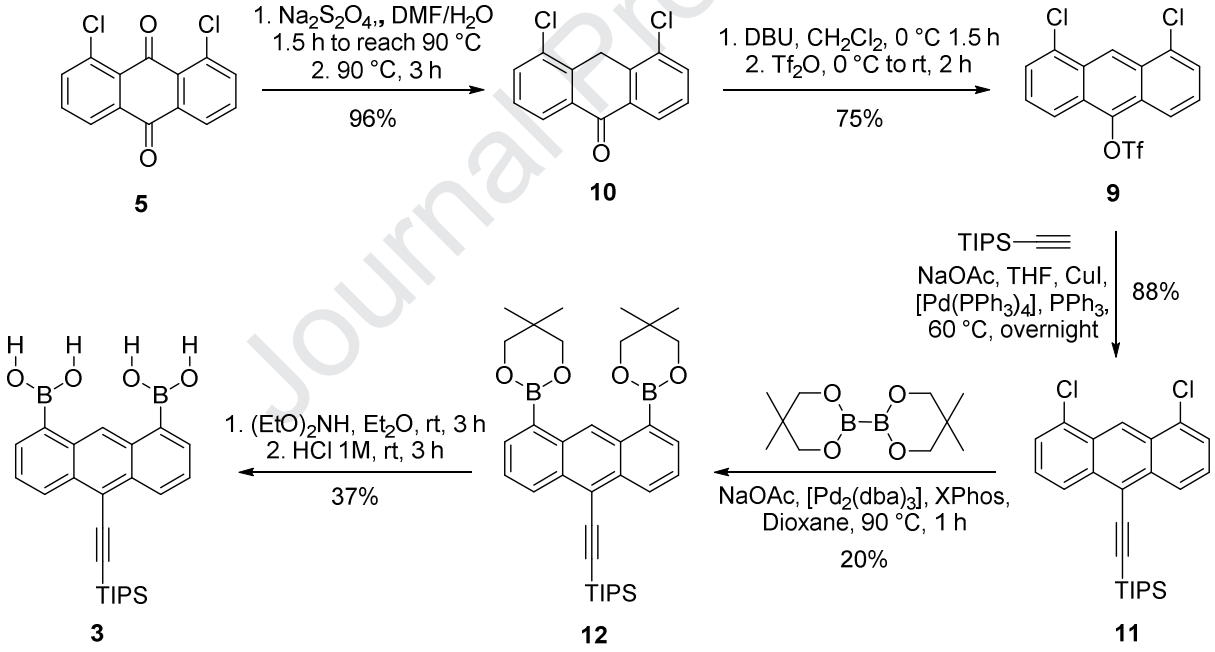

Scheme 2. Synthetic pathway to target molecule **3**.

The first synthetic step of this route involves the reduction of anthraquinone **5** to anthrone **10** with $Na_2S_2O_4$ (96% yield). The triflate insertion was obtained in 75% yield after deprotonation of anthrone **10** with DBU followed by the addition of Tf_2O. The structure of

anthracene **9** was confirmed by single crystal X-ray diffractions analysis (crystals obtained by slow evaporation of a $CHCl_3$ solution, Figure 4). The molecular packing is governed by the presence of π-π stacking as well as halogen-halogen interactions between chlorine and fluorine atoms. *Sonogashira*-type cross-coupling reaction between compound **9** and (triisopropylsilyl)acetylene (TIPSA) led to the formation of compound **11** in 88% yield. Following a similar protocol to that described previously for installing the boronic acid functionalities in molecules $\mathbf{2^R}$, target molecule **3** was obtained in moderate yield.

Figure 4. X-ray crystal structure of compound **9**; space group: C2/c. H atoms are omitted. Atom colours: green Cl, yellow S, pale green F, red O, grey C.

2.3 Study of the $Na_2S_2O_4$ reduction reaction of 1,8-dichloroanthraquinone.

While preparing the anthracenyl intermediates, the peculiar reduction conditions of 1,8-dichloroanthraquinone **5** with $Na_2S_2O_4$ stimulated our curiosity to shed further light on the mechanism of this reaction. In the literature, only a few studies address the challenge to unravel the mechanism of the $Na_2S_2O_4$-mediated reduction. In 1980 *Kellogg* and co-workers showed that, under basic conditions, $Na_2S_2O_4$ is an effective reagent for the reduction of aldehydes and ketones.[42] They suggested a two-step mechanism, in which an α-hydroxy sulfinate intermediate is formed followed by its reductive transformation with loss of SO_2. A similar mechanism was also proposed the year after by *Saito* and co-workers.[43] In 1996,

Müller and co-workers reported the regioselective reduction of *peri*-substituted anthraquinones into the relevant anthrones.[44] They hypothesised that the reduction undergoes formation of a diol intermediate that, in the presence of an acid, eliminates to give the relevant anthrone derivative. In a previous report, *Cristol* reported the rate of H_2O elimination from *cis*- and *trans*-9,10-anthraquinone diols. The author showed that the *syn* elimination, given by *trans* diols, is faster than that occurring with the *cis*-diols, with both diols being able to yield the relevant anthrone.[45] To commence, we prepared and isolated those reactive intermediates that, we think, are possibly lying on the reaction path to the anthrone product. In a first attempt, *peri*-substituted anthraquinone **5** was reacted with $Na_2S_2O_4$ at room temperature for 5 h (Scheme 3). Interestingly, under these reaction conditions intermediate 9-hydroxy-10-anthrone **13** was quantitatively obtained (structure confirmed by X-Ray diffraction analysis of crystals obtained through vapor diffusion of cyclohexane into a CH_2Cl_2 solution, Figure 5a).

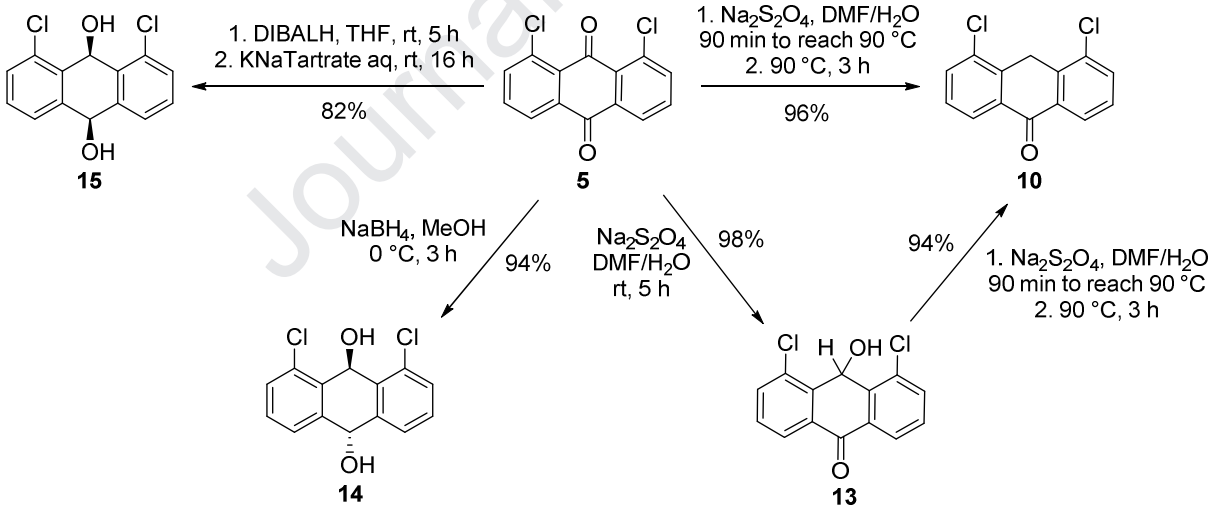

Scheme 3. Mechanistic study of the $Na_2S_2O_4$-mediated reduction of 1,8-dichloroanthraquinone to anthrone **10**: synthesis of the envisaged intermediates.

Successive reaction of **13** with $Na_2S_2O_4$ at 90 °C led to anthrone **10** in 94% yield, the structure of which could also be confirmed by X-ray diffraction (Figure 5b). These observations suggested that the $Na_2S_2O_4$-mediated reduction could occur stepwise, with the formation of 9-

hydroxy-10-anthrone in the first place, and of a diol anthraquinone in the later stage. To confirm this hypothesis, both *cis*- and *trans*- diols of 1,8-dichloroanthraquinone were also synthesized (Scheme 3). *trans*-Diol **14** was obtained by reaction of **10** in the presence of $NaBH_4$ in MeOH at 0 °C for 3 h, whereas *cis*-diol analogue **15** could be prepared in 82% yield using DIBALH in THF.

Figure 5. a) Crystal structure of compound **13**; space group: $P2_1/c$. **b)** Crystal structure of compound **10**; space group: $P\text{-}2_1$. H atoms are omitted except for OH and Csp_2H. Atom colours: green Cl, red O, grey C, white H.

The conformational properties of both 1,8-dichloroanthraquinone diols were confirmed by single-crystal X-Ray diffraction analyses. The structures of both diols were determined from crystals obtained by slow evaporation of acetone solutions (Figure 6a). Interestingly, molecules of *trans*-diol **14** arrange in a tape-like network through H-bonding interactions, connecting four neighbouring molecules ($O_1\square\square\square O_2$ = 2.867(4) Å and $O_1\square\square\square O_2$ = 2.926(4) Å). In this isomer, the two hydroxyl groups are in equatorial and axial positions, respectively.

On the other hand, the X-ray structure of *cis*-diol **15** shows the presence of the two hydroxyl groups in axial positions (Figure 6b) linked through an intramolecular H-bond ($O_1\square\square\square O_2$ = 2.876(3) Å). The molecules organise into dimers held together by two, squarely arranged H-bonds ($O_1\square\square\square O_2$ = 2.921(3) Å). *trans*- and *cis*-Diols **14** and **15** were used to unravel the possible elimination pathways leading to anthrone **10**.

Figure 6. a) Crystal structure of compound **14**; space group: $P2_1$. **b)** Crystal structure of compound **15**; space group: P-1. H atoms are omitted except for OH and Csp_2H. Atom colours: green Cl, red O, grey C, white H.

As the first experiment, the thermal elimination in DMF/H_2O at 90 °C for 5 h was attempted with *trans*- and *cis*-diols **14** and **15** (Table 1, entries 1&2). In both cases, no conversion was observed, which clearly suggest that heat alone is not sufficient for the reaction to occur. Therefore, we reacted independently *trans*- and *cis*-diols **14** and **15** in the presence of $Na_2S_2O_4$ at 90 °C for 5 h following the protocol conditions used to transform 1,8-dichloroanthraquinone **5** into anthrone **10**. Whereas *trans*-diol **14** did not yield any product, the reaction with *cis*-diol **15** led to the formation of anthrone **10** in 64% yield (Table 1, entries 3&4). This observation suggests that *cis*-diol **15** is likely the intermediate that, formed in the

$Na_2S_2O_4$-mediated reduction, allows the transformation of quinone **5** into anthrone **10**. When the diols are reacted independently in the presence of HCl at 90 °C for 5 h, both led to desired anthrone **10** quantitatively (Table 1, entries 5&6), as previously suggested by *Cristol*.

Table 1. Mechanistic study of the $Na_2S_2O_4$-mediated reduction of 1,8-dichloroanthraquinone to anthrone **10**: reduction attempts of diols **14** (*trans*) and **15** (*cis*).

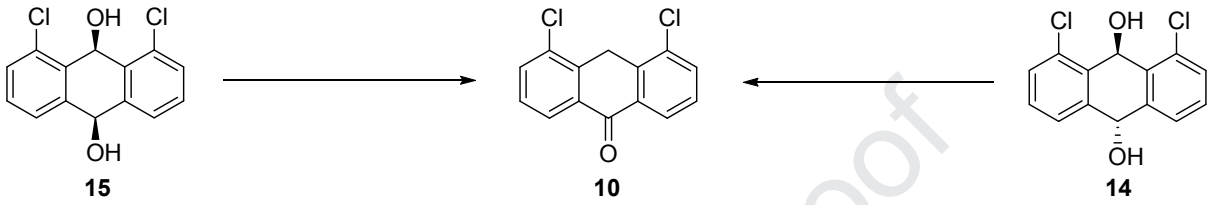

entry	Diol	Reagent	Solvent	Time	Temperature	Yield
1	**14**	-	DMF/H_2O	5 h	90 °C	0%
2	**15**	-	DMF/H_2O	5 h	90 °C	0%
3	**14**	$Na_2S_2O_4$	DMF/H_2O	5 h	90 °C	0%
4	**15**	$Na_2S_2O_4$	DMF/H_2O	5 h	90 °C	64%
5	**14**	HCl	DMF/H_2O	5 h	90 °C	96%
6	**15**	HCl	DMF/H_2O	5 h	90 °C	93%

Taken all together, these observations suggest that the $Na_2S_2O_4$-mediated reaction to anthrone **10** follows an antiperiplanar elimination pathway as only the *cis* isomer reacts under these reductive conditions (Scheme 4). Indeed, only *cis*-diol **15** can adopt a conformation suitable for an antiperiplanar elimination, i.e. hydrogen atom and hydroxyl group in *axial* positions. The elimination can occur through two different routes (Scheme 5). In route 1, a HSO_3^- anion, generated from thermal decomposition of $Na_2S_2O_4$, may deprotonate the axial hydrogen triggering an E_{1cb}-type elimination reaction (top, Scheme 5). In route 2, an antiperiplanar E_2-like elimination is proposed (down, Scheme 5). In both mechanistic propositions, a sulfinate

moiety is evoked as leaving group (possibly formed in the presence of $Na_2S_2O_4$ under refluxing conditions).

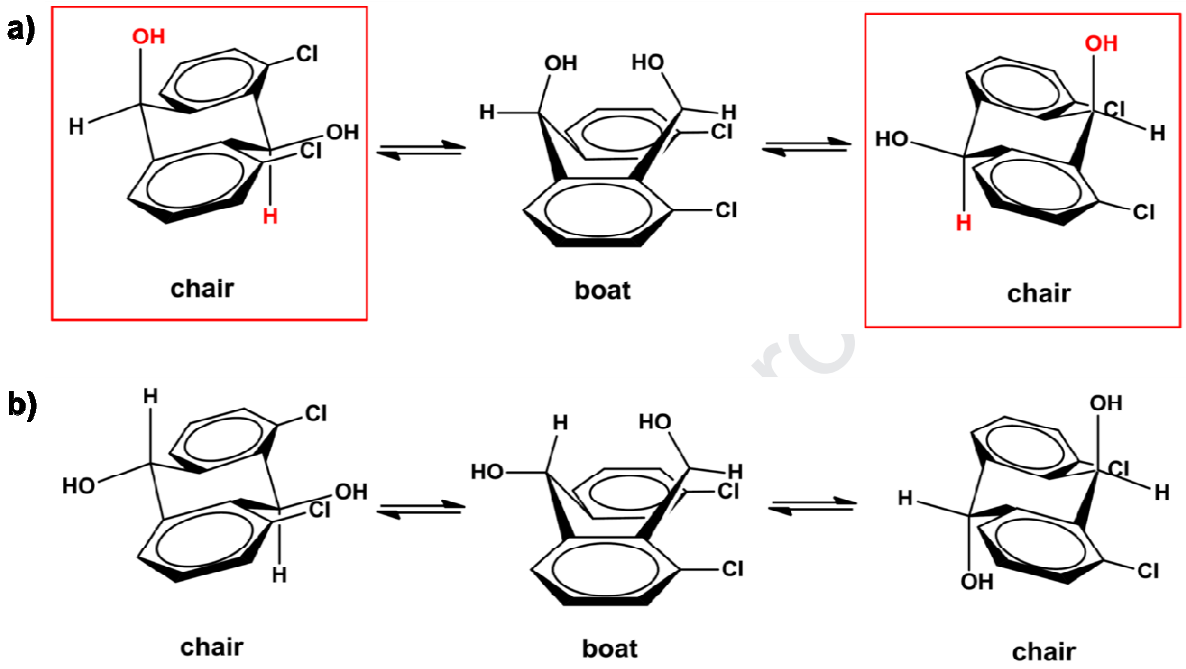

Scheme 4. Possible conformations of **a)** *cis*-diol **15** and **b)** *trans*-diol **14**. The red squares indicate the only conformation able to give antiperiplanar elimination.

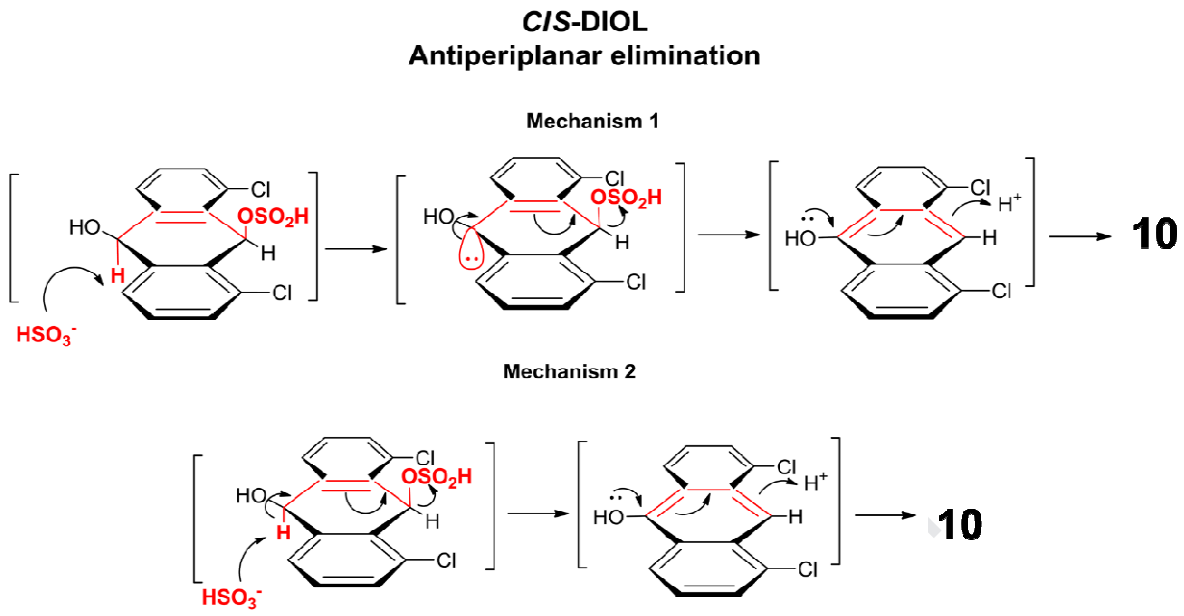

Scheme 5. Possible antiperiplanar elimination routes.

2.4 Homomolecular and heteromolecular hydrogen-bonding recognition properties.

2.4.1 H-bonding recognition at the solid state.

Suitable crystals of $\mathbf{2^{Me}}$ for X-ray diffraction analysis were obtained by vapor diffusion of H_2O into a DMSO solution (Figure 7a). In the solid state, molecule $\mathbf{2^{Me}}$ dimerizes into H-bonded complexes ($\mathbf{2^{Me}}$•$\mathbf{2^{Me}}$), in which each boronic acid moiety frontally engages into double DA-AD-type arrays (O_1□□□O_4 = 2.850(3) Å and O_2□□□O_3 = 2.787(3) Å) as *syn-anti* conformers.

Figure 7. a) X-ray crystal structure of compound $\mathbf{2^{Me}}$; space group: P-2_1/c. **b)** X-ray crystal structure of compound **3**; space group: C2/c. H atoms are omitted except for $B(OH)_2$. Atom colours: pink B, red O, pale yellow Si, yellow S, grey C, white H.

Notably, the *syn-anti* conformational preference of the hydroxyl groups forces the boronic acid moieties in the *peri*-positions to twist, and adopt a non-planar arrangement with the anthracene core (dihedral angles: O_1-B_1-C_1-C_2 = 58.9(3)°, O_2-B_1-C_1-C_{14} = 59.2(3)°, O_3-B_2-C_{11}-C_{12} = 38.1(4)° and O_4-B_2-C_{11}-C_{10} = 36.5(5)°). The arrangement of the boronic acids

observed in $\mathbf{2^{Me}}$ contrasts that observed for the boronate ester moieties in compound $\mathbf{8^{Me}}$, in which the boron-containing functionalities and the polycyclic aromatic skeleton are co-planar. Solvent molecules of DMSO are also present in the crystal, each H-bonded with the hydroxyl moieties of $\mathbf{2^{Me}}$ ($O_2\square\square\square O_8$ = 2.638(16) Å and $O_4\square\square\square O_7$ = 2.650(3) Å). Suitable crystals of molecule **3** were obtained by vapor diffusion of EtOH into a $CHCl_3$ solution (Figure 7b). As for molecule $\mathbf{2^{Me}}$, derivative **3** dimerizes into H-bonded complexes (**3●3**), in which each boronic acid moiety adopts a *syn-anti* conformation and frontally engages into double DA-AD-type H-bonding arrays ($O_1\square\square\square O_3$ = 2.781(3) Å and $O_2\square\square\square O_4$ = 2.787(4) Å). In contrast to the crystal packing of molecule $\mathbf{2^{Me}}$, each complex **3●3** establishes lateral H-bonds with adjacent dimers ($O_1\square\square\square O_3$ = 2.798(3) Å) forming a ladder-type network. As for $\mathbf{2^{Me}}$●$\mathbf{2^{Me}}$, the boronic acid moieties and the anthracenyl core adopt a non-planar conformation in dimer **3●3**.

2.4.2 Heteromolecular H-bonding recognition in solution.

At last, we attempted to study the formation of H-bonded heteromolecular complexes in solution using boronic acids derivatives ($\mathbf{2^{R}}$ and **3**) as the H-bonding DDDD partners and molecule **1** as the complementary AAAA-type acceptor. Due to the poor solubility of boronic acids $\mathbf{2^{Me}}$ and **3** in non-competitive organic solvents, any attempts to study their H-bonding recognition properties by ^{1}H-NMR titration failed. Thus we turned out attention to UV-vis absorption spectroscopy, and monitored any changes in the absorption profile of H-bonding acceptor **1** (c = 10^{-6} mol L^{-1} in CH_2Cl_2) upon increasing amount of H-bonding donor $\mathbf{2^{Me}}$ (Figure 8). As one can clearly notice in the absorption profiles shown in Figure 8, only a decrease in the intensity of the absorption bands characteristic of acceptor **1** (420 to 470 nm) was observed upon increasing addition (up to 0.5 equivalents) of donor $\mathbf{2^{Me}}$. No energy shifts

were observed for any of the electronic transitions. Further increases of the concentration of $\mathbf{2}^{\mathbf{Me}}$ (up to 3 equivalents) did not lead to any significant changes of the absorption envelop of acceptor **1**. If one considers that shifts in energy are frequently observed for the strongest absorption bands when a chromophore engages in H-bonding interactions in solution, we concluded that if a non-covalent complex is formed, this crashes out of solution (some precipitate was observed in the cuvette). H-bonding donor **3** displayed a similar behaviour to that of $\mathbf{2}^{\mathbf{Me}}$, whereas no spectral changes were observed when $\mathbf{2}^{\mathbf{TEG}}$ was used. Despite the numerous attempts, we could not grow suitable crystals for X-ray diffraction analysis of the H-bonded complexes ($\mathbf{2}^{\mathbf{Me}}\bullet\mathbf{1}$ and $\mathbf{3}\bullet\mathbf{1}$).

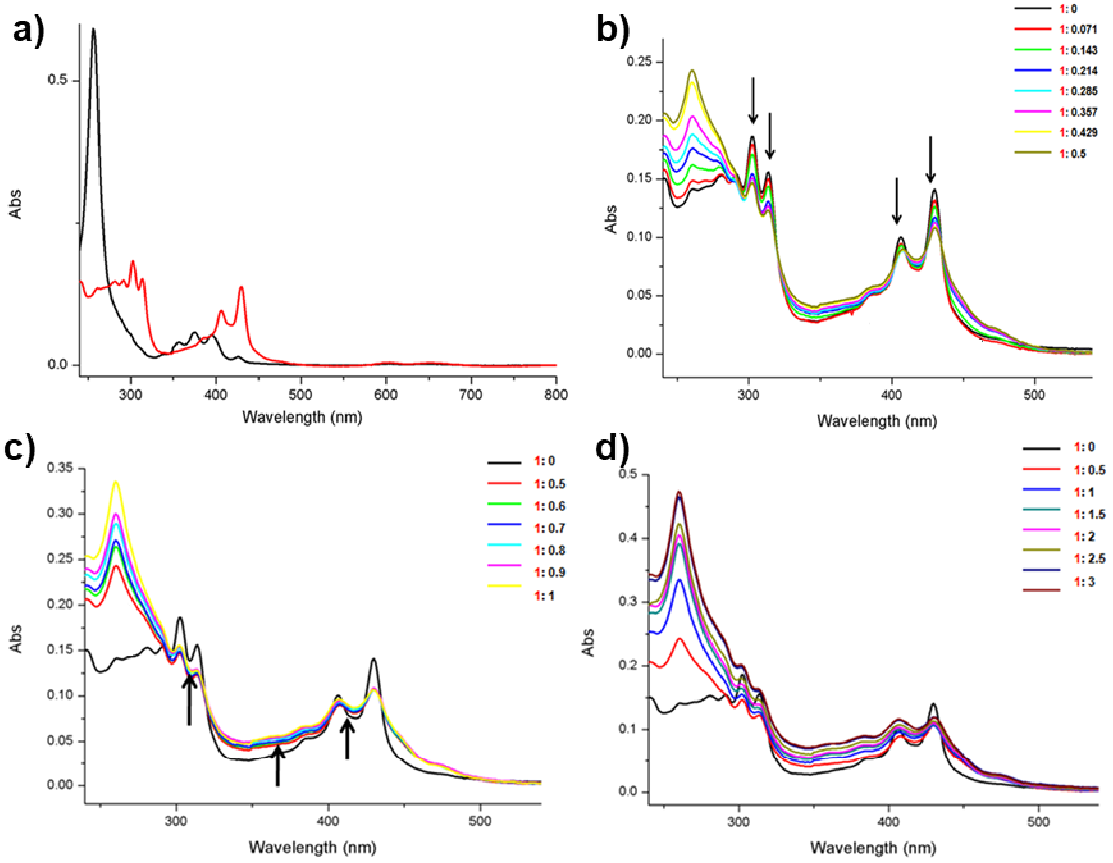

Figure 8. a) UV-vis absorption profiles of acceptor **1** (red) and donor $\mathbf{2^{Me}}$ (black) in CH_2Cl_2 at 10^{-6} M. **b)-d)** UV-Vis titration experiments in CH_2Cl_2 of acceptor **1** (10^{-6} M) with donor $\mathbf{2^{Me}}$ (the **1**:$\mathbf{2^{Me}}$ ratio is displayed in the legend).

Given the good solubility of H-bonding donor $\mathbf{2^{TEG}}$ in organic solvents, we studied the binding of $\mathbf{2^{TEG}}$ with **1** by means of ^{1}H-NMR titration. As peaks fingerprinting the boronic acid protons are generally not visible in $CDCl_3$,[31] a 1:1 mixture of C_6D_6 and THF-d_8 was first employed, but extensive precipitation occurred upon addition of both components to the solution. Instead, reduced precipitation was noticed with a 95:5 mixture of C_6D_6 and DMSO-d_6. Titration experiments were thus performed in the latter solvent mixture using H-bonding donor $\mathbf{2^{TEG}}$ and acceptor **1** as host and acceptor**,** respectively.

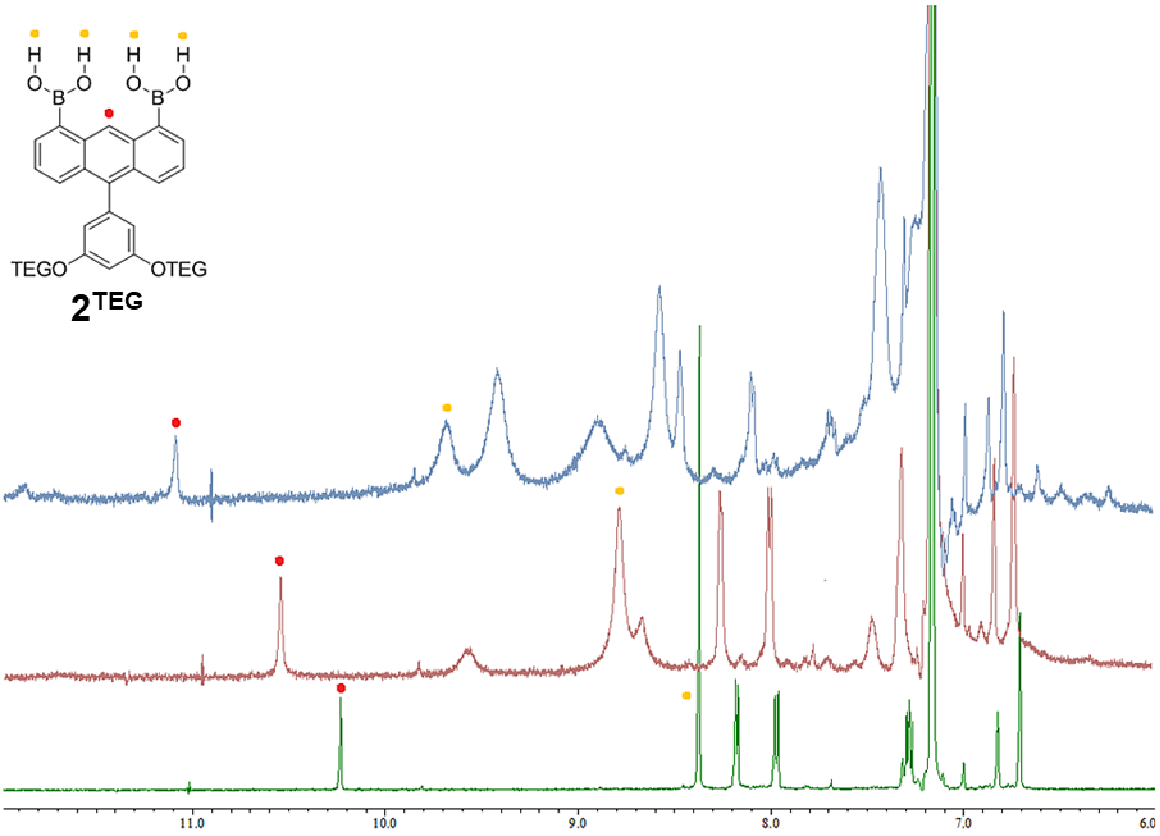

Figure 9. Selected regions of ^{1}H NMR titration experiments of H-bonding donor $\mathbf{2}^{\mathbf{TEG}}$ (5 mM) upon addition of H-bonding acceptor **1** (500 MHz, C_6D_6/DMSO-d_6 95/5, 298 K). The dots indicate the diagnostic proton resonances of H-bonding donor $\mathbf{2}^{\mathbf{TEG}}$. The molar ratios $\mathbf{2}^{\mathbf{TEG}}$:**1** of the different spectra are: 1:0 (bottom), 1:0.5 (middle), 1:1 (top).

Although some precipitation and peak broadening were observed during the titration experiments (Figure 9), addition of increasing amount of **1** to a 5 mM solution of $\mathbf{2}^{\mathbf{TEG}}$ led to noticeable downfield shift ($\Delta\delta = 1.31$ ppm) of the -B(O*H*)$_2$ proton resonances, suggesting the presence of H-bonding interactions. Together with the-B(O*H*)$_2$ resonances, also the peaks of the proton resonance of the aromatic *peri*-proton CH in position 9 revealed significant downfield shifts ($\Delta\delta = 0.49$ ppm) upon addition of **1**, confirming the presence of interactions involving the frontal boronic acid moieties. Unfortunately, the slight precipitation observed during the titration experiments together with the significant peak broadening (Figure 9) hampered any further attempts to produce meaningful thermodynamic data in solution.

3. Conclusion

In summary, herein we developed two synthetic pathways to prepare 1,8,10-trisubstituted anthracenes that, bearing two boronic acid functionalities, can act as multiple H-bonding donors. Whereas in the first approach the *peri*-substituted anthracenyl derivatives are synthesized through the addition of a Grignard nucleophile to 1,8-dichloroanthraquinone, in the second avenue a triflate-bearing 1,8,10-trisubstituted anthracene is prepared by $Na_2S_2O_4$ reduction of the anthraquinone into the anthrone precursor and functionalized through a metal-catalysed cross-coupling reaction. Complementary studies of the $Na_2S_2O_4$-mediated reduction of 1,8-dichloroanthraquinone allowed to shed further light on the mechanism leading to the anthrone intermediate, suggesting that the reaction possibly involves the formation of a *cis*-diol derivative that can undergo antiperiplanar elimination. X-ray diffraction investigations of the 1,8,10-trisubstituted anthracenyl boronic acids in the solid-state show that the molecules self-assemble into dimers through the formation of frontal H-bonds established between the *anti-syn* conformers of the boronic acid moieties. The binding properties of the boronic acids (DDDD) were also studied in solution in the presence of a suitable multiple H-bonding acceptor (AAAA), diisoquinolino[3,4-b:4',3'-g][1,8]naphthyridine. While UV-Vis spectroscopic investigations did not lead to any conclusive observations, ^{1}H-NMR titration experiments showed a significant downfield shift of the -B(O*H*)$_2$ proton resonances, suggesting the presence of H-bonding interactions. However, the poor solubility of the H-bonded complexes hampered precise determination of the stoichiometry of the complexes and of any thermodynamic parameters.

4. Experimental part

General Methods

Chemicals were purchased from *Sigma Aldrich, Acros Organics, Fluorochem, TCI, Carbosynth,* and *ABCR,* and were used as received. Solvents were purchased from *Sigma Aldrich* and *Acros Organics*. Deuterated solvents were purchased from *Eurisotop*. General solvents were distilled *in vacuo*. Anhydrous solvents such as Et_2O and THF were distilled from Na/benzophenone; CH_2Cl_2 from phosphorus pentoxide. Anhydrous DMF, 1,4-dioxane and MeOH were purchased and used without further purification. Anhydrous conditions were achieved by drying *Schlenk* lines, 2-neck flasks or 3-neck flasks by flaming with a heat gun under vacuum and purging with argon. The inert atmosphere was maintained using argon-filled balloons equipped with a syringe and needle that was used to penetrate the silicon stoppers used to close the flasks' necks. The addition of liquid reagents was done by means of dried plastic syringes or by cannulation. **Column chromatography** was carried out using *Grace* silica gel 60 (particle size 40-63 μm). **Melting points** (m.p.) were measured on a *Büchi Melting Point B-545*. All of the melting points have been measured in open capillary tubes and have not been corrected. **Nuclear magnetic resonance** (NMR) ^{1}H and ^{13}C spectra were obtained on a 400 MHz NMR *(Jeol JNM EX-400).* Chemical shifts were reported in ppm according to tetramethylsilane using the solvent residual signal as an internal reference ($CDCl_3$: ^{1}H = 7.26 ppm, ^{13}C = 77.16 ppm, CD_2Cl_2: ^{1}H = 5.32 ppm, ^{13}C = 53.84 ppm, CD_3OD: ^{1}H = 3.10 ppm, ^{13}C = 49.00 ppm, DMSO-d_6: ^{1}H = 2.50 ppm, ^{13}C = 39.52 ppm, $(CD_3)_2CO$: ^{1}H = 2.05 ppm, ^{13}C = 29.84 ppm). Coupling constants (*J*) were given in Hz. Resonance multiplicity was described as *s* (singlet), *d* (doublet), *t* (triplet), *q* (quartet). Carbon spectra were acquired with a complete decoupling for the proton. All spectra were recorded at 25 °C. **Infrared spectra** (IR) were recorded on a *Perkin-Elmer Spectrum II FT-IR System UATR*, mounted with a diamond crystal. Selected absorption bands are reported in wavenumber (cm^{-}

[1]). **Mass spectrometry** was generally performed by the *Fédération de Recherche ICOA/CBM (FR2708) platform* of Orléans in France. High-resolution ESI mass spectra (HRMS) were performed on a *Bruker maXis Q-TOF* in the positive ion mode. The analytes were dissolved in a suitable solvent at a concentration of 1 mg/mL and diluted 200 times in methanol (≈ 5 ng/mL). The diluted solutions (1μL) were delivered to the ESI source by a *Dionex Ultimate 3000 RSLC* chain used in FIA (Flow Injection Analysis) mode at a flow rate of 200 μL/min with a mixture of CH_3CN/H_2O + 0.1% of HCO_2H (65/35). ESI conditions were as follows: capillary voltage was set at 4.5 kV; dry nitrogen was used as nebulizing gas at 0.6 bars and as drying gas set at 200 °C and 7.0 L/min. ESI-MS spectra were recorded at 1 Hz in the range of 50-3000 *m/z*. Calibration was performed with ESI-TOF Tuning mix from Agilent and corrected using lock masses at *m/z* 299.294457 (methyl stearate) and 1221.990638 (HP-1221). Data were processed using *Bruker DataAnalysis 4.1* software. MALDI-MS were performed by the *Centre de spectrométrie de masse* at the *Université de Mons* and recorded using a *Waters QToF Premier* mass spectrometer equipped with a nitrogen laser, operating at 337 nm with a maximum output of 500 mW delivered to the sample in 4 ns pulses at 20 Hz repeating rate. Time-of-flight mass analyses were performed in the reflectron mode at a resolution of about 10,000. The matrix solution (1 μL) was applied to a stainless-steel target and air dried. Analyte samples were dissolved in a suitable solvent to obtain 1 mg/ml solutions. 1 μL aliquots of those solutions were applied onto the target area already bearing the matrix crystals, and air dried. For the recording of the single-stage MS spectra, the quadrupole (rf-only mode) was set to pass ions from 100 to 1000 Th, and all ions were transmitted into the pusher region of the time-of-flight analyser where they were analyzed with 1 s integration time.

10-(3,5-dimethoxyphenyl)anthracene-1,8-diyl)diboronic acid 2^{Me}

To a suspension of compound **8^{Me}** (100 mg, 0.186 mmol) in Et_2O (9.6 mL), a solution of diethanolamine (40 µL, 0.409 mmol) in *i*-PrOH (2 mL) was added. The mixture was stirred for 3 h at room temperature and the solution filtered. The solid was suspended in 1M *aq* HCl (6.4 mL). The mixture was stirred at room temperature for 3 h, filtered and the solid washed with H_2O (3×5 mL). The solid was dried using a freeze-dryer overnight to yield compound **2^{Me}** (73 mg, 98%) as a bright yellow powder. M.p. 276-277°C. FTIR (ATR) ν (cm^{-1}): ν 3375, 1590, 1381, 1201, 1150, 1061, 1030, 992, 755, 739. ^{1}H-NMR (400 MHz, DMSO-d_6): δ 9.43 (s, 1H), 8.35 (s, 4H), 7.64 (d, *J* = 6.0 Hz, 2H), 7.56 (d, *J* = 8.7 Hz, 2H), 7.36 (t, *J* = 7.6 Hz, 2H), 6.70 (s, 1H), 6.46 (s, 2H), 3.79 (s, 6H). ^{13}C-NMR (100 MHz, DMSO-d_6): δ 160.5, 141.0, 136.6, 136.1, 132.6, 130.8, 129.2, 128.7, 126.9, 124.9, 109.1, 99.0, 55.3. ^{11}B-NMR (128 MHz, DMSO-d_6): δ 30.7. HRMS (ESI): m/z $[M + H]^+$ Calcd for $C_{22}H_{21}B_2O_6$ 403.1526; Found 403.1523.

(10-(3,5-bis(2-(2-(2-methoxyethoxy)ethoxy)ethoxy)phenyl)anthracene-1,8-diyl)diboronic acid 2^{TEG}

In a dry Schlenk, compound **7^{TEG}** (169 mg, 0.261 mmol), bis(neopentyl glycolato)diboron (146 mg, 0.644 mmol), XPhos (10 mg, 0.0208 mmol) and NaOAc (270 mg, 3.3 mmol) were added in 1,4-dioxane (4.5 mL). The resulting suspension was degassed through 3 freeze-pump-thaw cycles and $[Pd_2(dba)_3]$ (14 mg, 0.016 mmol) added to the mixture. The reaction was stirred at 90 °C for 1.5 h. The solvent was removed *in vacuo*. The catalyst was precipitated upon addition of toluene, removed through filtration on celite and the filtrate concentrated. To a solution of the resulting crude mixture in Et_2O (9.6 mL), a solution of diethanolamine (40 µL, 0.409 mmol) in *i*-PrOH (2 mL) was added. The mixture was stirred for 2 h at room temperature. The solution was washed by centrifugation upon addition of Et_2O (4×8 mL) and a solid isolated. The solid was suspended in 1M *aq* HCl (6.4 mL). The mixture

was stirred at room temperature for 2 h. The solid was washed by centrifugation upon addition of H_2O (4×8 mL) and a solid isolated. The solid was dried using a freeze-dryer overnight, yielding compound **2**$^{\mathbf{TEG}}$ (64 mg, 37%) as a white powder. M.p. 113-115°C. FTIR (ATR) ν (cm^{-1}): ν 3344, 2875, 1587, 1429, 1166, 1093, 826. ^{1}H-NMR (400 MHz, DMSO-d_6): δ 9.42 (s, 1H), 8.37 (s, 4H), 7.64 (d, *J* = 6.5 Hz, 2H), 7.57 (d, *J* = 8.8 Hz, 2H), 7.36 (dd, *J* = 8.8, 6.5 Hz, 2H), 6.73 (s, 1H), 6.44 (d, *J* = 2.1 Hz, 2H), 4.13 (t, *J* = 4.2 Hz, 4H), 3.73 (t, *J* = 4.2 Hz, 4H), 3.58-3.56 (m, 4H), 3.52-3.48 (m, 8H), 3.41- 3.38 (m, 4H), 3.20 (s, 6H). ^{13}C-NMR (100 MHz, DMSO-d_6): δ 170.9, 159.7, 141.0, 132.6, 130.8, 128.7, 126.9, 124.9, 109.7, 99.9, 71.3, 70.0, 69.8, 69.6, 69.0, 67.4, 58.12 carbon missing probably due to overlap). ^{11}B-NMR (128 MHz, DMSO-d_6): not detected. HRMS (ESI): m/z $[M + Na]^+$ Calcd for $C_{34}H_{44}B_2NaO_{12}$ 689.2922 Found 689.2921.

(10-((triisopropylsilyl)ethynyl)anthracene-1,8-diyl)diboronic acid 3

To a suspension of compound **12** (90 mg, 0.1545 mmol) in Et_2O (8 mL), a solution of diethanolamine (33 µL, 0.337 mmol) in *i*-PrOH (1.7 mL) was added. The mixture was stirred for 3 h at room temperature. The suspension was filtered and the solid obtained suspended in 1M *aq* HCl (6.4 mL). The mixture was stirred at room temperature for 3 h. The solution was filtered and the solid washed with H_2O (3×5 mL). The solid was dried using a freeze-dryer overnight, yielding desired compound **3** (25 mg, 37%) as a bright yellow powder. M.p. 292-293 °C. FTIR (ATR) ν (cm^{-1}): ν 3326, 2940, 2863, 1366, 1326, 1239, 1115, 1032, 882, 748, 662. ^{1}H-NMR (400 MHz, DMSO-d_6): δ 9.54 (s, 1H), 8.50 (d, *J* = 8.5 Hz, 2H), 8.44 (s, 4H), 7.74 (d, *J* = 6.2 Hz, 2H), 7.64 (t, *J* = 8.5 Hz, 2H), 1.24 (s, 21H). ^{13}C-NMR (100 MHz, DMSO-d_6): δ 132.5, 131.9, 131.6, 131.4, 126.6, 126.4, 115.8, 101.7, 18.7, 10.9 (2 carbon missing probably due to overlap). ^{11}B-NMR (128 MHz, DMSO-d_6): δ 31.3. HRMS (ESI): m/z $[M + H]^+$ Calcd for $C_{25}H_{33}B_2O_4Si$ 447.2338; Found 447.2336.

1,8-dichloro-10-(3,5-dimethoxyphenyl)-10-hydroxyanthracen-9(10H)-one 6

In a dry 2 neck flask, 1-bromo-3,5-dimethoxybenzene **4** (108.5 mg, 0.5 mmol) was dissolved in dry THF (2 mL). 0.5 mL of the resulting solution were added to a second dry two neck flask containing Mg (14 mg, 0.575 mmol) and a crystal of I_2. The suspension was heated up (around 60 °C) until reaching a point in which a transparent suspension was obtained (the iodine disjunction). As soon as no suspension was observed, the rest of the solution containing **4** was added to the solution. The mixture was stirred for 1 h at room temperature. The resulting Grignard suspension was added to a dry two neck flask containing an ice-cold solution of compound **5** (138.5 mg, 0.5 mmol) dissolved in dry THF (3 mL). The reaction was let to reach room temperature stirring overnight. The solvent was removed *in vacuo* and compound **6** was purified by silica gel column chromatography (Cyclohexane/EtOAc 75:25) as a white solid (139 mg, 67%). M.p. 232-233 °C. FTIR (ATR) ν (cm^{-1}): ν 1677, 1587, 1244, 1192, 1151, 1134, 974, 788, 722. ^{1}H-NMR (400 MHz, $CDCl_3$): δ 7.79-7.76 (m, 2H), 7.46-7.44 (m, 4H), 6.35 (d, *J* = 2.2 Hz, 2H), 6.24 (t, *J* = 2.2 Hz, 1H), 3.66 (s, 6H). ^{13}C-NMR (100 MHz, $CDCl_3$): δ 183.4, 161.0, 148.1, 147.4, 133.0, 131.5, 130.5, 124.7, 104.3, 99.2, 74.1, 55.5 (1 peak missing, probably due to overlap).

1,8-dichloro-10-(3,5-dimethoxyphenyl)anthracene 7^{Me}

In a dry 30 mL Schlenk containing a suspension of $LiAlH_4$ (44 mg, 1.152 mmol) in dry Et_2O (4.5 mL) and cooled down at 0 °C was added $BF_3.Et_2O$ (0.329 mL, 2.6 mmol). A solution of **6** (133 mg, 0.48 mmol) in dry CH_2Cl_2 (4.5 mL) was added and the mixture stirred at reflux for 48 h. After cooling using an ice-bath, MeOH (4 mL), H_2O (2 mL) and CH_2Cl_2 (10 mL) were added. The phases were separated, and the aqueous phase extracted with CH_2Cl_2 (2×5 mL). The combined organic layers were washed with brine (10 mL), dried over $MgSO_4$ and filtered. The solvent was removed *in vacuo* and compound $\mathbf{7^{Me}}$ purified by silica gel column

chromatography (Pentane/EtOAc 98:2) as a pale yellow solid (188 mg, 95%). M.p. 224-225°C. FTIR (ATR) ν (cm^{-1}): ν 1592, 1359, 1154, 845, 814, 123, 697. ^{1}H-NMR (400 MHz, $CDCl_3$): δ 9.39 (s, 1H), 7.67 (d, *J* = 8.9 Hz, 2H), 7.63 (d, *J* = 7.3 Hz, 2H), 7.32-7.28 (m, 2H), 6.66-6.65 (m, 1H), 6.56-6.55 (m, 2H), 3.83 (s, 6H). ^{13}C-NMR (100 MHz, $CDCl_3$): δ 160.9, 140.4, 138.5, 132.7, 131.3, 129.2, 126.4, 126.0, 125.6, 121.1, 109.3, 100.1, 55.6. HRMS (ESI): m/z $[M]^+$ Calcd for $C_{22}H_{16}O_2Cl_2$ 382.0527; Found 382.0515.

10-(3,5-bis(2-(2-(2-methoxyethoxy)ethoxy)ethoxy)phenyl)-1,8-dichloro anthracene 7^{TEG}

In a dry Schlenk, compound $\mathbf{7^{Me}}$ (70 mg, 0.182 mmol) was dissolved in dry CH_2Cl_2 (3 mL) and cooled down at -78 °C. BBr_3 (0.5 mL, 0.5 mmol, 1 M in hexane) cooled at -78 °C was added at this temperature. The solution was let to reach room temperature overnight, poured into ice water and extracted with EtOAc (3×5 mL). The organic layers were combined, dried over $MgSO_4$, filtered and evaporated. The residue was precipitated in pentane. In a dry Schlenk, 50 mg of the solid obtained, TEG-OTs (107.5 mg, 0.338 mmol) and K_2CO_3 (77.2 mg, 0.56 mmol) were added to dry DMF (1 mL). The reaction was stirred at 50 °C for 48 h. The mixture was diluted with H_2O (6 mL) and the aqueous suspension extracted with CH_2Cl_2 (3×12 mL). The combined organic layers were dried over $MgSO_4$ and the solvent removed *in vacuo*. Compound $\mathbf{7^{TEG}}$ was purified through silica gel column chromatography (EtOAc/MeOH 99:1) as a brown viscous oil (55 mg, 61%). M.p. 53-54 °C. FTIR (ATR) ν (cm^{-1}): ν 2872, 1592, 1434, 1350, 1169, 1100, 1064, 845, 815. ^{1}H-NMR (400 MHz, $CDCl_3$): δ 9.36 (s, 1H), 7.64-7.60 (m, 4H), 7.28-7.26 (m, 2H), 6.67 (s, 1H), 6.54 (d, *J* = 2.0 Hz, 2H), 4.13 (t, *J* = 4.7 Hz, 4H), 3.85 (t, *J* = 4.7 Hz, 4H), 3.74-3.71 (m, 4H), 3.68-3.65 (m, 4H), 3.64-3.60 (m, 4H), 3.53-3.50 (m, 4H), 3.34 (s, 6H). ^{13}C-NMR (100 MHz, $CDCl_3$): δ 160.0, 140.2, 138.5, 132.6, 131.2, 129.2, 126.5, 126.0, 125.6, 121.1, 110.2, 101.3, 72.0, 71.0, 70.8, 70.7,

69.8, 67.8, 59.2. HRMS (MALDI-TOF): m/z $[M]^+$ Calcd for $C_{34}H_{40}O_8Cl_2$ 646.2100; Found 646.2095.

2,2'-(10-(3,5-dimethoxyphenyl)anthracene-1,8-diyl)bis(5,5-dimethyl-1,3,2-dioxaborinane) 8^{Me}

In a dry Schlenk, compound **7^{Me}** (100 mg, 0.261 mmol), bis(neopentyl glycolato)diboron (146 mg, 0.644 mmol), XPhos (10 mg, 0.0208 mmol) and NaOAc (270 mg, 3.3 mmol) were added in 1,4-dioxane (4.5 mL). The resulting suspension was degassed through 3 freeze-pump-thaw cycles and $[Pd_2(dba)_3]$ (14 mg, 0.016 mmol) added to the mixture. The reaction was stirred at 90 °C for 1 h. The solvent was removed *in vacuo.* The catalyst was precipitated by addition of toluene and removed through filtration on celite. The filtrate was concentrated and precipitation in Et_2O yielded compound **8^{Me}** as a light-yellow powder (80 mg, 57%). M.p. 292-293 °C. FTIR (ATR) ν (cm^{-1}): ν 1584, 1283, 1248, 1138, 752, 675. ^{1}H-NMR (400 MHz, $CDCl_3$): δ 10.26 (s, 1H), 8.03 (d, *J* = 6.0 Hz, 2H), 7.76 (d, *J* = 8.7 Hz, 2H), 7.31 (dd, *J* = 8.7, 6.6 Hz, 2H), 6.64-6.60 (m, 1H), 6.56-6.55 (m, 2H), 3.98 (s, 8H), 3.81 (s, 6H), 1.17 (s, 12H). ^{13}C-NMR (100 MHz, $CDCl_3$): δ 160.7, 142.1, 137.3, 134.3, 134.1, 129.8, 129.5, 128.3, 124.5, 109.6, 99.7, 90.2, 72.8, 55.6, 32.1, 22.3. ^{11}B-NMR (128 MHz, $CDCl_3$): 27.0.

4,5-dichloroanthracen-9-yl trifluoromethanesulfonate 9

In a dry 50 mL flask containing a suspension of compound **10** (200 mg, 0.763 mmol) in CH_2Cl_2 (4.2 mL), DBU (228.6 µl, 1.527 mmol) was added dropwise over a period of 90 min (26 µL every 10 min). Trifluoromethanesulfonic anhydride (0.954 mmol, 160.5 µL, 1M in CH_2Cl_2) was slowly added over a period of 90 min (110 µL every 10 min). The reaction was stirred at 0 °C for 10 min, after which additional trifluoromethanesulfonic anhydride (200 µL) was added and the reaction stirred for 45 min. H_2O (3 mL) was added to the reaction vessel and the resulting mixture stirred overnight. The phases were separated, and the aqueous layer

extracted with CH_2Cl_2 (3×20 mL). The organic layers were combined, dried over $MgSO_4$, filtered and evaporated. The resulting crude was purified through silica gel column chromatography (CH_2Cl_2/Cyclohexane 1:1) to yield compound **9** as a crystalline yellow solid (227 mg, 75%). M.p. 123-125 °C. FTIR (ATR) ν (cm^{-1}): ν 1398, 1323, 1207, 1126, 891, 801, 726, 727. ^{1}H-NMR (400 MHz, $CDCl_3$): δ 9.39 (s, 1H), 8.16 (d, *J* = 8.9 Hz, 2H), 7.71 (d, *J* = 7.3 Hz, 2H), 7.58 (dd, *J* = 8.9, 7.3 Hz, 2H). ^{13}C-NMR (100 MHz, $CDCl_3$): δ 140.2, 133.1, 129.6, 128.1, 126.9, 125.9, 122.6, 120.5 (carbon bearing the fluorine atoms missing). HRMS (ESI): m/z $[M + H]^+$ Calcd for $C_{15}H_8O_3SF_3Cl_2$ 394.9517; Found 394.9512.

4,5-dichloroanthracen-9(10H)-one 10

In a 500 mL 2 neck flask, compound **5** (2.77 g, 9.99 mmol) was suspended in DMF (100 mL) and H_2O (100 mL). The resulting mixture was heated at 30 °C and $Na_2S_2O_4$ (1.739 g, 99.9 mmol) was added under argon. Every 15 min the temperature was raised by 10 °C, reaching 90 °C in 1.5 h. The reaction was stirred at 90 °C for 3 h. The mixture was cooled down at room temperature and CH_2Cl_2 (100 mL) was added. The phases were separated and the aqueous layer extracted with CH_2Cl_2 (1×200 mL; 2×150 mL). The organic layers were collected, dried over $MgSO_4$, filtered and evaporated. The crude material was purified through silica gel column chromatography (CH_2Cl_2/Cyclohexane 1:1), to yield compound **10** as a white crystalline solid (2.533 g, 96%). M.p. 187-189 °C. FTIR (ATR) ν (cm^{-1}): ν 1656, 1589, 1308, 1283, 1133, 818, 740. ^{1}H-NMR (400 MHz, $CDCl_3$): δ 8.29 (dd, *J* =7.8, 1.1 Hz, 2H), 7.71 (dd, *J* =7.8,1.1 Hz, 2H), 7.46 (t, *J* = 7.8, 2H), 4.25 (s, 2H). ^{13}C-NMR (100 MHz, $CDCl_3$): δ 182.9, 137.5, 134.3, 133.9, 133.0, 128.2, 126.5, 29.6. HRMS (ESI): m/z $[M + H]^+$ Calcd for $C_{14}H_9OCl_2$ 263.0024; Found 263.0026. Spectral characterization agrees with previously reported data.[46,47]

((4,5-dichloroanthracen-9-yl)ethynyl)diisopropyl(methyl)silane 11

In a dry Schlenk containing a suspension of compound **9** (980 mg, 2.49 mmol) and NaOAc (2.577 g, 31.41 mmol) in THF (70 mL), CuI (47.5 mg, 0.249 mmol) and PPh_3 (261.24 mg, 0.996 mmol) were added. 3 freeze-pump-thaw cycles were performed and [$Pd(PPh_3)_4$] (288 mg, 0.249 mmol) added at room temperature. After an additional freeze-pump-thaw cycle triisopropylacetylene (614.5 μL, 2.739 mmol) was added and the reaction stirred at 60 °C overnight. The solvent was removed *in vacuo*. The crude material was purified through silica gel column chromatography (Cyclohexane) to yield **11** as a crystalline yellow solid (936 mg, 88%). M.p. 169-171°C. FTIR (ATR) ν (cm^{-1}): ν 2941, 2864, 1441, 1339, 1146, 994, 880, 736, 677. ^{1}H-NMR (400 MHz, $CDCl_3$): δ 9.26 (s, 1H), 8.55 (d, *J* = 8.5 Hz, 2H), 7.64 (d, *J* = 7.1 Hz, 2H), 7.50 (dd, *J* = 8.5, 7.1 Hz, 2H), 1.26 (s, 21H). ^{13}C-NMR (100 MHz, $CDCl_3$): δ 134.1, 133.1, 129., 126.9, 126.4, 126.2, 121.9, 119.5, 104.6, 102.7, 19.0, 11.6. HRMS (ESI): m/z [M + H]$^+$ Calcd for $C_{25}H_{29}SiCl_2$ 427.1410; Found 427.1406.

((4,5-bis(5,5-dimethyl-1,3,2-dioxaborinan-2-yl)anthracen-9-yl)ethynyl) triisopropylsilane 12

In a dry Schlenk, compound **11** (556 mg, 1.300 mmol), bis(neopentyl glycolato)diboron (725 mg, 3.211 mmol), XPhos (50 mg, 0.104 mmol) and NaOAc (1.345 g, 16.400 mmol) were added in dry 1,4-dioxane (4.5 mL). The resulting suspension was degassed through 3 freeze-pump-thaw cycles and [$Pd_2(dba)_3$] (14 mg, 0.016 mmol) added to the mixture. The reaction was stirred at 90 °C for 1 h. The solvent was removed *in vacuo.* The catalyst was precipitated upon addition of toluene and removed through filtration on celite. The filtrate was concentrated *in vacuo.* A white powder was precipitated upon addition of *n*-hexane and removed through filtration on celite. The solvent was removed *in vacuo,* yielding the desired compound **12** (151 mg, 20%) as a pale-yellow powder. M.p. 97-100 °C. FTIR (ATR) ν (cm^{-1}): ν 2957, 2933, 1417, 1385, 1341, 1289, 1249, 1142, 663. ^{1}H-NMR (400 MHz, $CDCl_3$): δ 10.25

(s, 1H), 8.73 (d, *J* = 8.5 Hz, 2H), 8.08 (d, *J* = 6.6 Hz, 2H), 7.54 (t, *J* = 8.5 Hz, 2H), 3.97 (s, 8H), 1.27-1.26 (m, 21H), 1.16 (s, 12H). ^{13}C-NMR (100 MHz, $CDCl_3$): δ 134.8, 134.1, 132.7, 131.8, 129.7, 125.9, 104.4, 88.9, 72.8, 32.1, 22.3, 19.1, 11.7 (2 peaks missing probably due to overlap). ^{11}B-NMR (128 MHz, $CDCl_3$): δ 27.63.

4,5-dichloro-10-hydroxyanthracen-9(10H)-one 13

In a 500 mL flask containing a suspension of compound **5** (2.77 g, 9.99 mmol) in DMF (100 mL) and H_2O (100 mL), $Na_2S_2O_4$ (1.739 g, 99.9 mmol) was added under argon. The reaction was stirred at room temperature overnight. The solvent was removed *in vacuo*. The crude was dissolved in CH_2Cl_2 (200 mL) and H_2O (100 mL) added. The phases were separated and the aqueous layer was extracted with CH_2Cl_2 (3×150 mL). The organic layers were combined, dried over $MgSO_4$, filtered and evaporated. The crude material was purified through silica gel column chromatography (CH_2Cl_2/Cyclohexane 1:1), to yield compound **13** as an orange powder (2.56 g, 98%). M.p. 202-205 °C. FTIR (ATR) ν (cm^{-1}): ν 3513, 1657, 1574, 1309, 1132, 1000, 791, 753, 721. ^{1}H-NMR (400 MHz, $CDCl_3$): δ 8.20 (dd, *J* = 8.0, 1.1 Hz, 2H), 7.73 (dd, *J* = 7.8, 1.1 Hz, 2H), 7.50 (dd, *J* = 8.0, 7.8 Hz, 2H), 6.39 (s, 1H) (OH signal missing). ^{13}C-NMR (100 MHz, $CDCl_3$): δ 182.7, 138.4, 135.1, 135.0, 132.8, 130.2, 126.7, 61.8. HRMS (ESI): m/z $[M + H]^+$ Calcd for $C_{14}H_9O_2Cl_2$ 278.9974; Found: 278.9970.

(9r,10r)-1,8-dichloro-9,10-dihydroanthracene-9,10-diol 14

In a two necked flask under argon, a solution of compound **5** (400 mg, 1.433 mmol) in dry MeOH (7.2 mL) was cooled to 0 °C and $NaBH_4$ (217 mg, 5.732 mmol) was added in small portions in order to prevent the temperature to rise. The resulting mixture was stirred between 0-5 °C for 1 h. The crude was poured into ice water and desired compound **14** precipitated as a white powder, filtered off and washed with H_2O (363 mg, 90%). M.p. 157-160 °C. FTIR (ATR) ν (cm^{-1}): ν 3403, 1449, 1192, 959, 869, 786, 692. ^{1}H-NMR (400 MHz, CD_3OD): δ

7.74 (dd, *J* = 7.2, 1.0 Hz, 2H), 7.39-7.36 (m, 4H), 6.66 (s, 1H), 5.87 (s, 1H) (OH signal missing). ^{13}C-NMR (100 MHz, CD_3OD): δ 146.4, 134.8, 134.6, 130.2, 129.1, 124.5, 67.9, 64.4. HRMS (ESI): m/z $[M + Na]^+$ Calcd for $C_{14}H_{10}Cl_2NaO_2$ 302.9950; Found 302.9945.

(9s,10s)-1,8-dichloro-9,10-dihydroanthracene-9,10-diol 15

To a solution of 1,8-dichloroanthracene-9,10-dione **5** (277 mg, 1 mmol) in dry THF (30 mL) was added dropwise DIBAH (3 mL, 3 mmol, 1 M in hexane). The reaction mixture was stirred for 5 h, followed by the addition of saturated aqueous Rochelle's salt solution (25 mL). The resulting mixture was stirred at room temperature overnight. The mixture was extracted with EtOAc (3×25 mL), the organic layers were combined, dried over $MgSO_4$, filtered and evaporated. Compound **15** was purified through silica gel column chromatography (Cyclohexane/EtOAc 8:2) and isolated as a white powder (252 mg, 89%). M.p. 207-210 °C. FTIR (ATR) ν (cm^{-1}): ν 3346, 1661, 1581, 1451, 1176, 955, 810, 763. ^{1}H-NMR (400 MHz, CD_3OD): δ 7.49-7.44 (m, 4H), 7.36 (t, *J* = 7.8 Hz, 2H), 6.37 (s, 1H), 5.51 (s, 1H) (OH signals missing). ^{13}C-NMR (100 MHz, CD_3OD): δ 142.7, 137.3, 135.4, 130.8, 130.6, 129.2, 71.3, 64.3. HRMS (ESI): m/z $[M]^+$ Calcd for $C_{14}H_{10}Cl_2NaO_2$ 302.9950; 302.9950.

Acknowledgments

D.B. gratefully acknowledge the EU through the SGt-ERC (project: COLORLANDS), MSCA-RISE (project: INFUSION), MSCA-ITN (project PHOTOTRAIN), IA-H2020 (project: DecoChrom) funding schemes for the financial support. A.S. thanks the DecoChrom project for his post-doctoral fellowship.

Supporting Information

Synthetic pathways and protocol for compound **1**, DFT explanations, ^{1}H, ^{13}C and ^{11}B NMR spectra, and crystallographic data. This material is available free of charge via the Internet.

References

1. Hall, D. G. *Boronic Acids: Preparation and Applications in Organic Synthesis and Medicine*: Weinheim, Germany, 2005.
2. Suzuki, A. *Angew. Chem., Int. Ed.* 2011; *50*: 6722.
3. Mora, M.; Jimenez-Sanchidrian, C.; Ruiz, J. R. *Curr. Org. Chem.* 2012; *16*: 1128.
4. Lennox, A. J. J.; Lloyd-Jones, G. C. *Chem. Soc. Rev.* 2014; *43*: 412.
5. Heravi, M. M.; Malmir, M.; Moradi, R. *Curr. Org. Chem.* 2019; *23*: 2469.
6. Nishiyabu, R.; Kubo, Y.; James, T. D.; Fossey, J. S. *Chem. Commun.* 2011; *47*: 1106.
7. Sun, X.; James, T. D. *Chem. Rev.* 2015; *115*: 8001.
8. Brooks, W. L. A.; Sumerlin, B. S. *Chem. Rev.* 2016; *116*: 1375.
9. Akgun, B.; Hall, D. G. *Angew. Chem., Int. Ed.* 2018; *57*: 13028.
10. Rowan, S. J.; Cantrill, S. J.; Cousins, G. R. L.; Sanders, J. K. M.; Stoddart, J. F. *Angew. Chem., Int. Ed.* 2002; *41*: 898.
11. Lehn, J.-M. *Chem. Soc. Rev.* 2007; *36*: 151.
12. Jin, Y.; Yu, C.; Denman, R. J.; Zhang, W. *Chem. Soc. Rev.* 2013; *42*: 6634.
13. Wilson, A.; Gasparini, G.; Matile, S. *Chem. Soc. Rev.* 2014; *43*: 1948.
14. Fournier, J.-H.; Maris, T.; Wuest, J. D.; Guo, W.; Galoppini, E. *J. Am. Chem. Soc.* 2003; *125*: 1002.
15. Maly, K. E.; Malek, N.; Fournier, J.-H.; Rodriguez-Cuamatzi, P.; Maris, T.; Wuest, J. D. *Pure Appl. Chem.* 2006; *78*: 1305.
16. Adamczyk-Wozniak, A.; Cyranski, M. K.; Dabrowska, A.; Gierczyk, B.; Klimentowska, P.; Schroeder, G.; Zubrowska, A.; Sporzynski, A. *J. Mol. Struct.* 2009; *920*: 430.

17. Regueiro-Figueroa, M.; Djanashvili, K.; Esteban-Gomez, D.; de Blas, A.; Platas-Iglesias, C.; Rodriguez-Blas, T. *Eur. J. Org. Chem.* 2010: 3237.

18. Cyranski, M. K.; Klimentowska, P.; Rydzewska, A.; Serwatowski, J.; Sporzynski, A.; Stepien, D. K. *CrystEngComm* 2012; *14*: 6282.

19. Adamczyk-Wozniak, A.; Brzozka, Z.; Dabrowski, M.; Madura, I. D.; Scheidsbach, R.; Tomecka, E.; Zukowski, K.; Sporzynski, A. *J. Mol. Struct.* 2013; *1035*: 190.

20. Campos-Gaxiola, J. J.; Vega-Paz, A.; Roman-Bravo, P.; Hopfl, H.; Sanchez-Vazquez, M. *Cryst. Growth Des.* 2010; *10*: 3182.

21. Rettig, S. J.; Trotter, J. *Can. J. Chem.* 1977; *55*: 3071.

22. Cyranski, M. K.; Jezierska, A.; Klimentowska, P.; Panek, J. J.; Sporzynski, A. *J. Phys. Org. Chem.* 2008; *21*: 472.

23. Durka, K.; Jarzembska, K. N.; Kamiński, R.; Luliński, S.; Serwatowski, J.; Woźniak, K. *Cryst. Growth Des.* 2013; *13*: 4181.

24. Adamczyk-Wozniak, A.; Cyranski, M. K.; Durka, K.; Gozdalik, J. T.; Klimentowska, P.; Rusiecki, R.; Sporzynski, A.; Zarzeczanska, D. *Crystals* 2019; *9*: 109.

25. Rodríguez-Cuamatzi, P.; Vargas-Díaz, G.; Höpfl, H. *Angew. Chem., Int. Ed.* 2004; *43*: 3041.

26. Pedireddi, V. R.; SeethaLekshmi, N. *Tetrahedron Lett.* 2004; *45*: 1903.

27. SeethaLekshmi, S.; Varughese, S.; Giri, L.; Pedireddi, V. R. *Cryst. Growth Des.* 2014; *14*: 4143.

28. TalwelkarShimpi, M.; Oeberg, S.; Giri, L.; Pedireddi, V. R. *Cryst. Growth Des.* 2017; *17*: 6247.

29. Rodriguez-Cuamatzi, P.; Luna-Garcia, R.; Torres-Huerta, A.; Bernal-Uruchurtu, M. I.; Barba, V.; Hopfl, H. *Cryst. Growth Des.* 2009; *9*: 1575.

30. Campillo-Alvarado, G.; Brannan, A. D.; Swenson, D. C.; MacGillivray, L. R. *Org. Lett.* 2018; *20*: 5490.

31. Georgiou, I.; Kervyn, S.; Rossignon, A.; De Leo, F.; Wouters, J.; Bruylants, G.; Bonifazi, D. *J. Am. Chem. Soc.* 2017; *139*: 2710.

32. Djurdjevic, S.; Leigh, D. A.; McNab, H.; Parsons, S.; Teobaldi, G.; Zerbetto, F. *J. Am. Chem. Soc.* 2007; *129*: 476.

33. Leigh, D. A.; Robertson, C. C.; Slawin, A. M. Z.; Thomson, P. I. T. *J. Am. Chem. Soc.* 2013; *135*: 9939.

34. Blight, B. A.; Hunter, C. A.; Leigh, D. A.; McNab, H.; Thomson, P. I. T. *Nat. Chem.* 2011; *3*: 244.

35. Sijbesma, R. P.; Meijer, E. W. *Chem. Commun.* 2003: 5.

36. Wilson, A. J. *Soft Matter* 2007; *3*: 409.

37. Beijer, F. H.; Kooijman, H.; Spek, A. L.; Sijbesma, R. P.; Meijer, E. W. *Angew. Chem., Int. Ed.* 1998; *37*: 75.

38. Zimmerman, S. C.; Corbin, P. S. *Struct. Bonding* 2000; *96*: 63.

39. Sijbesma, R. P.; Beijer, F. H.; Brunsveld, L.; Folmer, B. J. B.; Hirschberg, J. H. K. K.; Lange, R. F. M.; Lowe, J. K. L.; Meijer, E. W. *Science* 1997; *278*: 1601.

40. Marangoni, T.; Bonifazi, D. *Nanoscale* 2013; *5*: 8837.

41. Wada, T.; Muckerman, J. T.; Fujita, E.; Tanaka, K. *Dalton Trans.* 2011; *40*: 2225.

42. De Vries, J. G.; Kellogg, R. M. *J. Org. Chem.* 1980; *45*: 4126.

43. Gassman, P. G.; Rasmy, O. M.; Murdock, T. O.; Saito, K. *J. Org. Chem.* 1981; *46*: 5455.

44. Prinz, H.; Wiegrebe, W.; Mueller, K. *J. Org. Chem.* 1996; *61*: 2853.

45. Cristol, S. J. *Acc. Chem. Res.* 1971; *4*: 393.

46. Karama, U.; Sultan, M. A.; Ghabour, H. A.; Fun, H. K.; Kh. Warad, I. *Z. Kristallogr. - New Cryst. Struct.* 2013; *228*: 405.

47. Tauchert, M. E.; Kaiser, T. R.; Goethlich, A. P. V.; Rominger, F.; Warth, D. C. M.; Hofmann, P. *ChemCatChem* 2010; *2*: 674.

Declaration of interests

☒ The authors declare that they have no known competing financial interests or personal relationships that could have appeared to influence the work reported in this paper.

☐The authors declare the following financial interests/personal relationships which may be considered as potential competing interests: